Advances in materials science of concrete at IPPT PAN – short review

Michal A. Glinicki

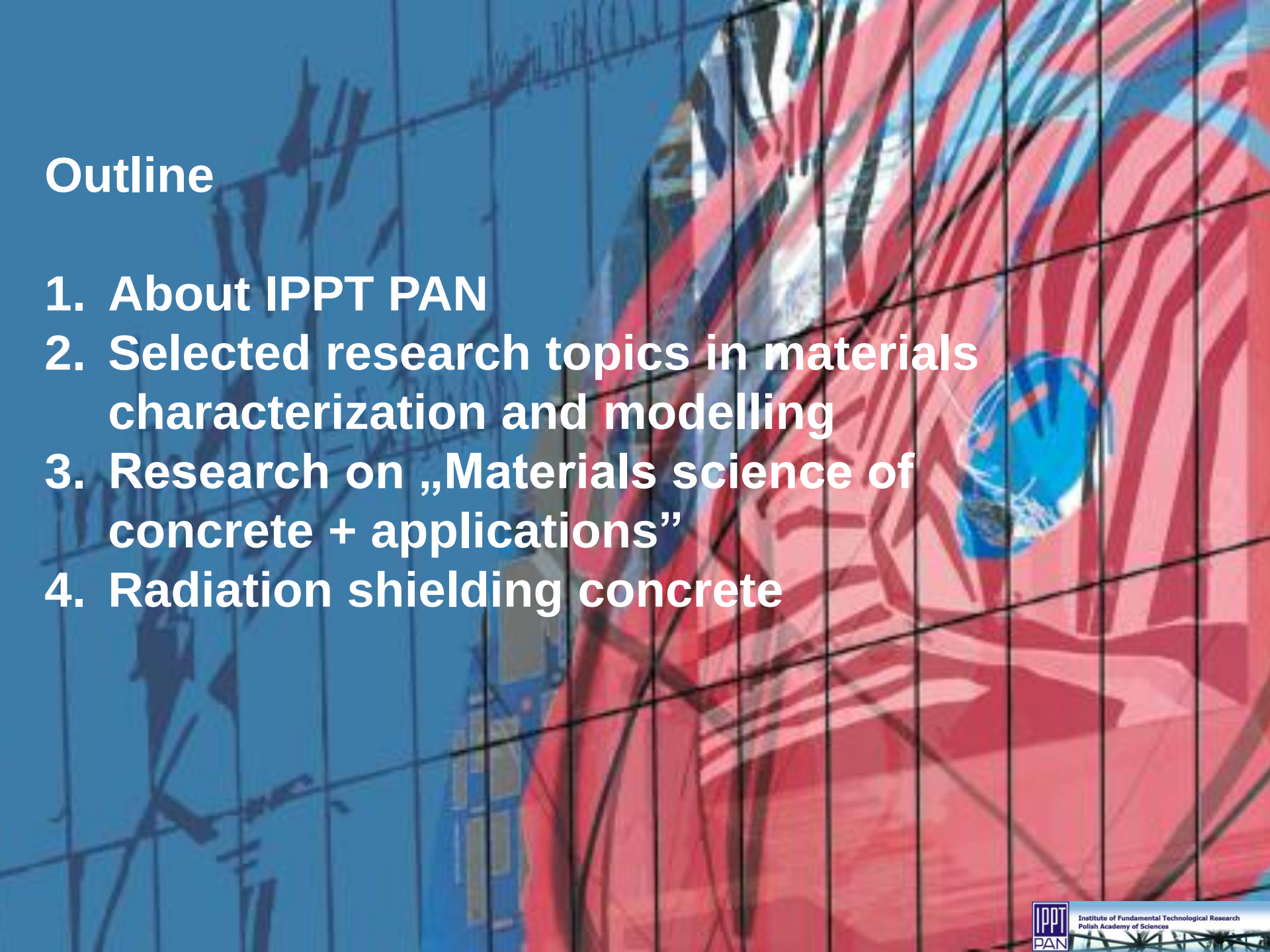

Outline

1. About IPPT PAN
2. Selected research topics in materials characterization and modelling
3. Research on „Materials science of concrete + applications”
4. Radiation shielding concrete

Activity area of IPPT PAN

Institute of Fundamental Technological Research

founded in 1953 as a part of the Polish Academy of Sciences

- The main task : to conduct **engineering research** in the selected areas which are the focus of the world's science and technology.
- The principal research fields:
theoretical and applied mechanics, mechanics of structures, materials science, fluid mechanics, applied informatics, acoustoelectronics, ultrasonic medical diagnostics and biomechanics.
- Funding of research:
government funding; EU and other research projects; industry

Organizational structure of IPPT PAN

Research staff: about 120 researchers (incl. 15 full professors, 26 associate professors and 46 senior researchers with the Ph.D.)

Seven Departments:

- Experimental Mechanics
- Mechanics of Materials
- Intelligent Technologies
- Ultrasound
- Theory of Continuous Media
- Information and Computational Science
- Biosystems and Soft Matter

Postgraduate PhD studies

Modelling of advanced composite materials

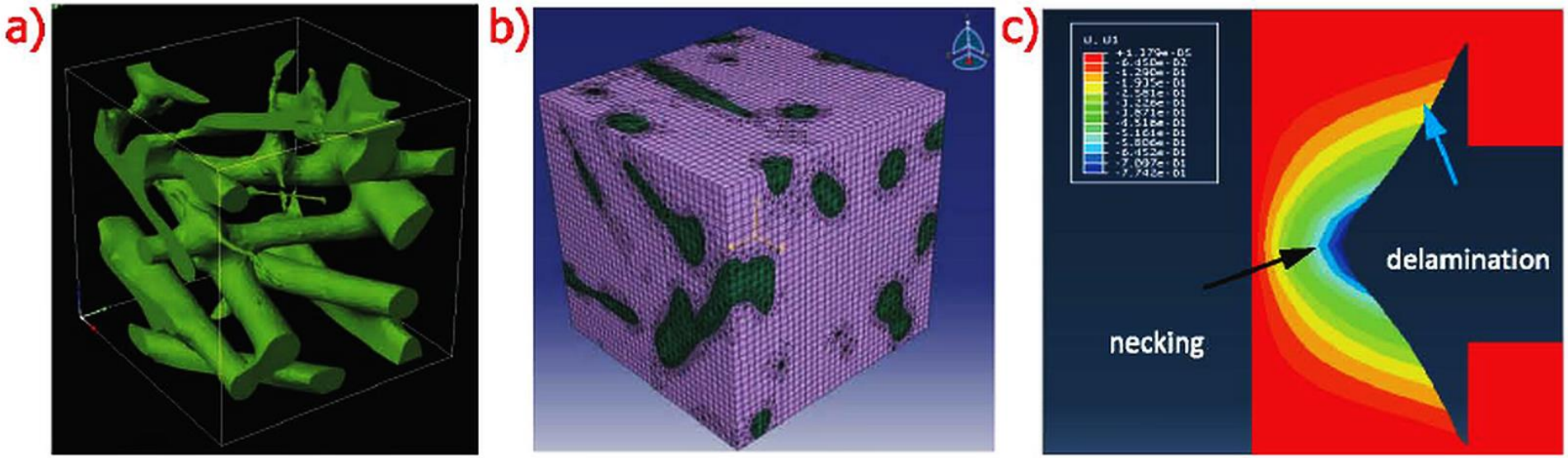

a) Micro-CT image of interpenetrating phase composite created with SimplewareScaniP/FE software
b) ABAQUS finite element model mesh
c) modelling of crack bridging by metal ligament in metal-ceramic interpenetrating phase composites: radial displacement distribution

Thin surface layers by ion implantation

The implanted gradient layers are constituted of shape memory alloys, high speed steels or Ti- alloys. Microstructure, implanted ions distribution and mechanical properties of modified layers are investigated. The goal is an optimal selection of process parameters for different materials.

a)

b)

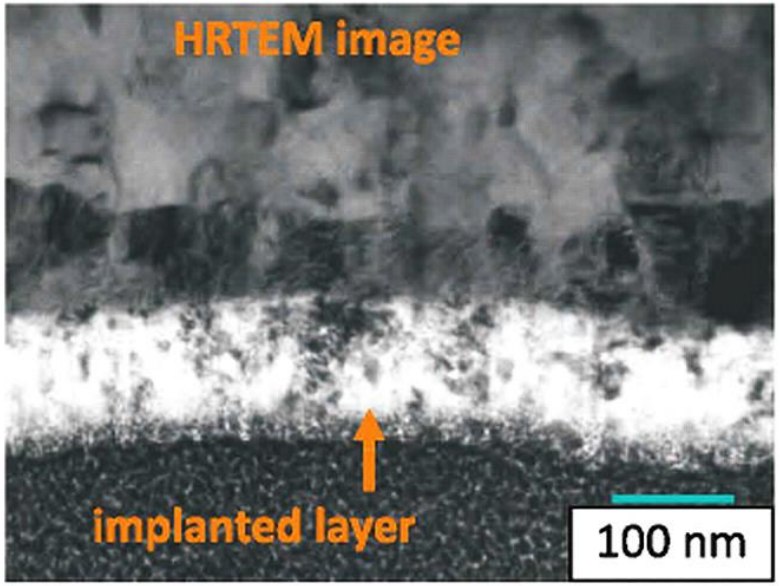

a) Ion implanter, b) morfology of implanted layer.

Identification of material properties using nanoindentation

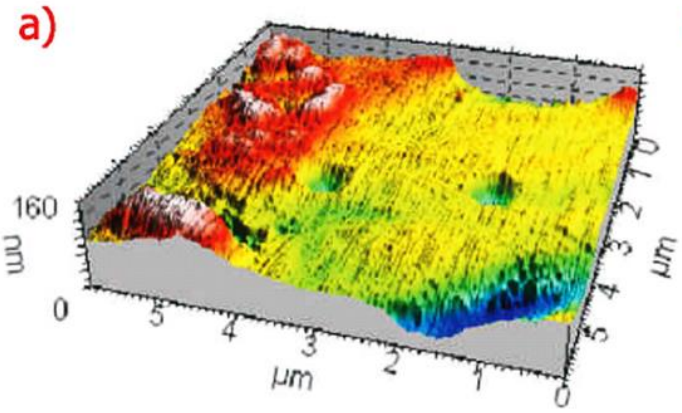

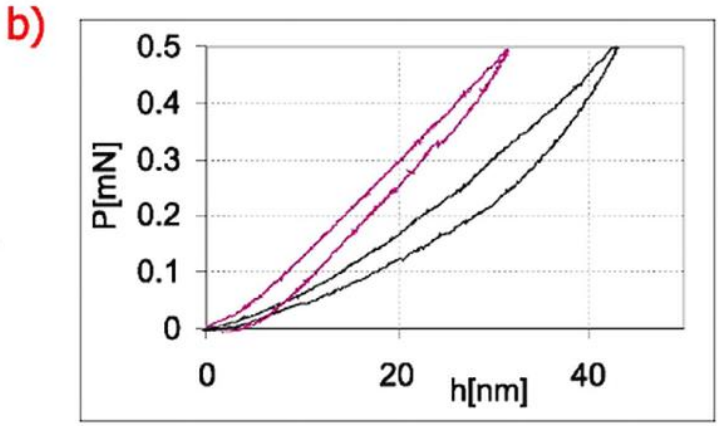

a) Effect of nanoindentation tests in the metal phase of sintered metal-ceramics composite (Mo+40%Al_2O_3).
b) Nanoindentation curves for ion implanted (red) andnon-implanted (black) shape-memory NiTi alloy.

Tests of inelastic materials in a wide range of strain rates

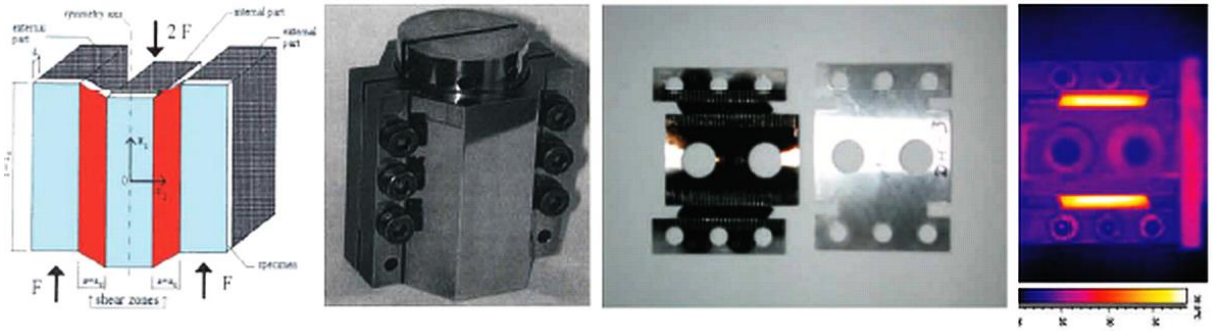

Upper: Set-up for shear compression tests and examples of investigated shear compression specimens.
Lower: Double shear testing set implemented for dynamic tests of metal sheets with use of IR thermography.

Numerical models for simulations of biomechanical phenomena

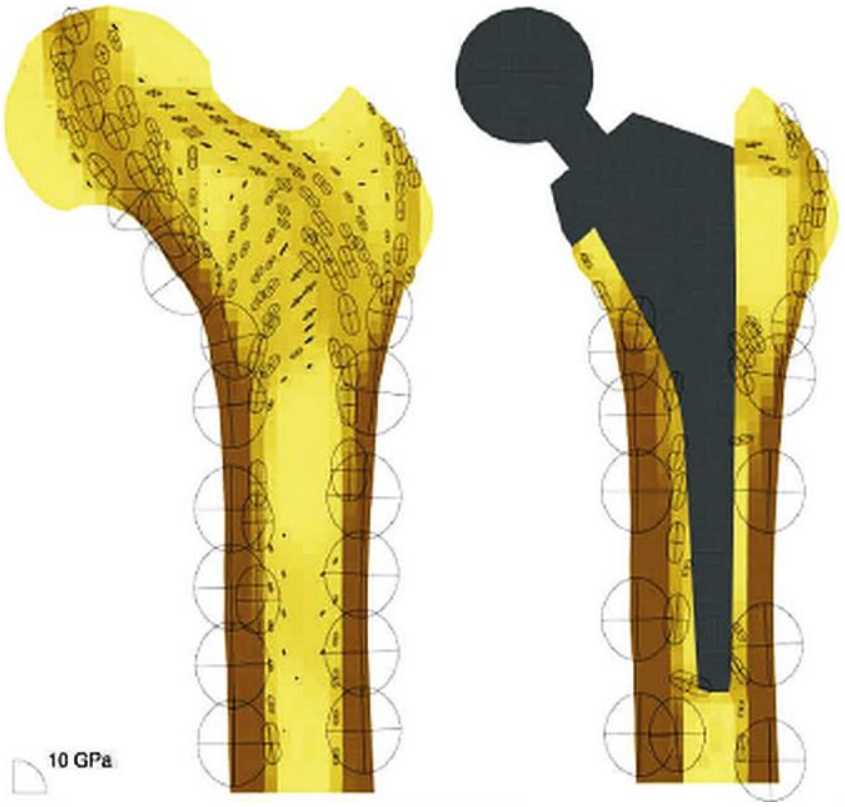

Parametric model of cancellous bone treated as porous material with repeatable microstructure.

Distribution of bone density and elastic anisotropy as a result of simulation of adaptive tissue remodelling in femur (without and with endoprosthesis).

Research on materials science of concrete

Division of Materials Science in Construction Engineering
Head: M.A. Glinicki
Staff: 7 permament + temporary up to 20 for larger projects

- Development of multi-component materials for sustainable construction
- Experimental evaluation of microstructure, micromechanical properties and durability of cement - based composites
- Design of high performance materials exposed to combined action of environmental loads, mechanical loads and nuclear radiation
- Optimization of dispersed fibre reinforcement and fibre-matrix contact properties

Related research topics at IPPT PAN

- ❑ Characterization of new SCMs from ‘clean coal’ energy production; development of new cements
- ❑ Quantitative characterization of micostructure (voids, cracks, delaminations, gradient properties)
- ❑ Transport properties and durability of concrete in aggressive environment and radiation exposure
- ❑ Micromechanical approach to long-term toughness of fiber reinforced concrete
- ❑ Identification of thermal/rheological properties of hardening concrete
- ❑ Soft computing methods (machine learning) for discovery of composition-properties relations

Highly active coal ash from clean combustion

Non-standard coal ash in Poland – up to 10 mln ton/year

Circulating Fluidized-bed Combustion Technology (CFBC)

- fuel flexibility (low-grade coal, biomass, sludge, waste plastics, and waste tires as fuel)

- SOx emissions significantly decreased -desulfurization intrafurnace, using mainly limestone

- low combustion temperature 850 to 900°C, thereby suppressing thermal NOx emissions

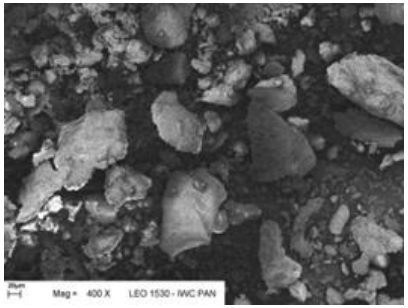

CFBC fly ash = residuum from burning and desulphurization process in CFBC boilers.

Phase composition of cement paste with CFBC fly ash

XRD: Intensity of ettringite peak [counts]

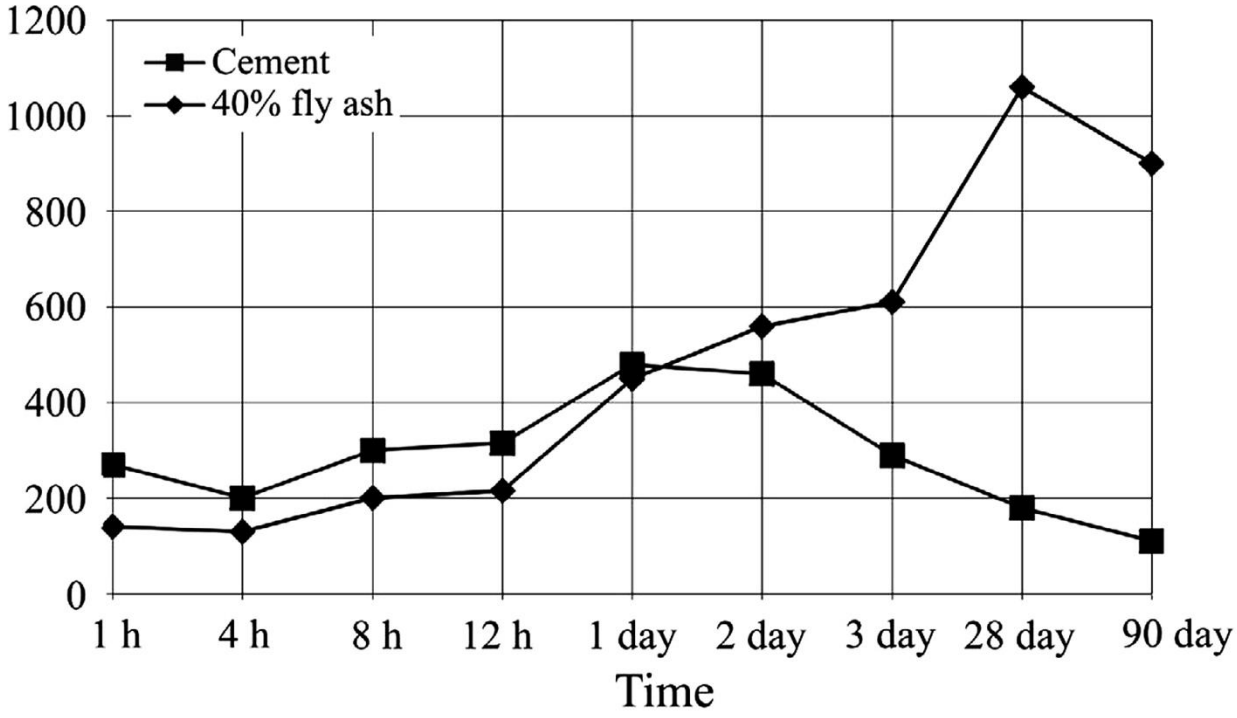

Significantly increased content of crystalline ettringite at later ages
Reason: increased content of anhydrite in CFBC fly ash

CFBC fly ash beneficiation: mechanical activation of particles by impacts

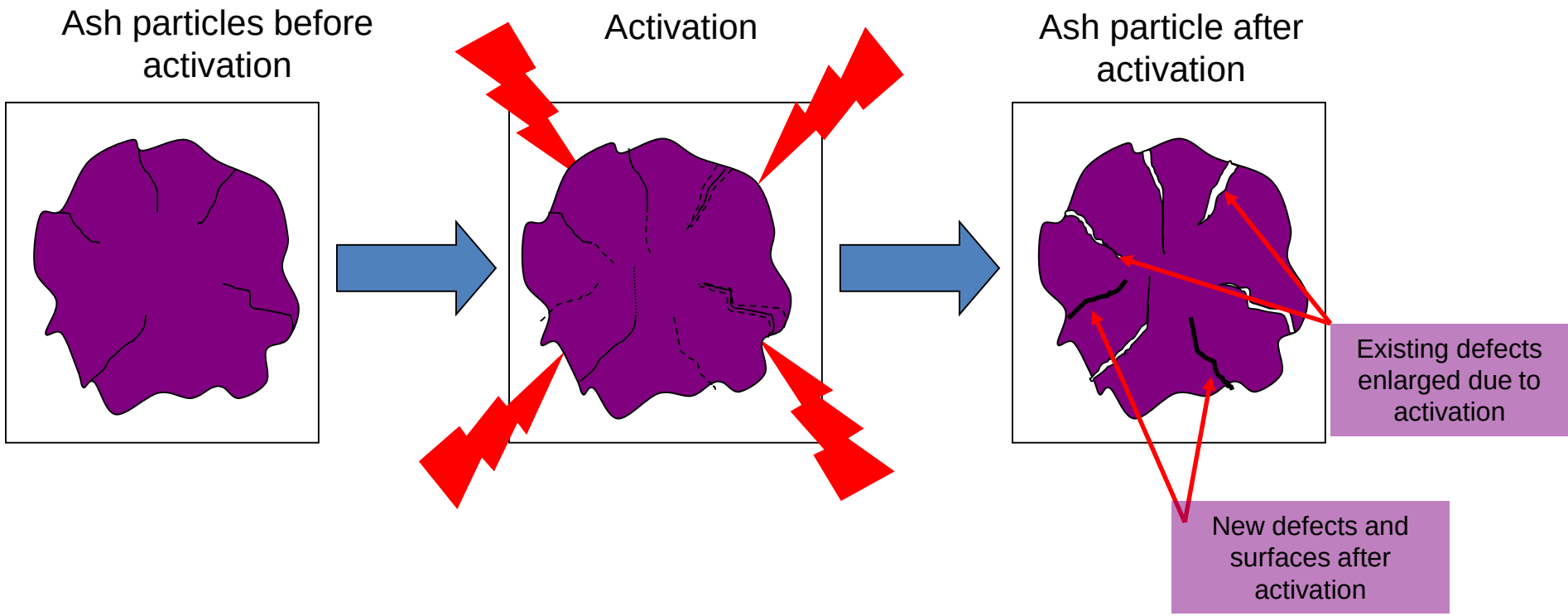

Strength efficiency of activated CFBC fly ash: greater than 1.0
i.e. greater than Portland cement

Characterization of high calcium fly ash (HFCA)

Particles:
spherical 1-50 μm; irregular and aggregates 20-100 μm
solid and plerospheres

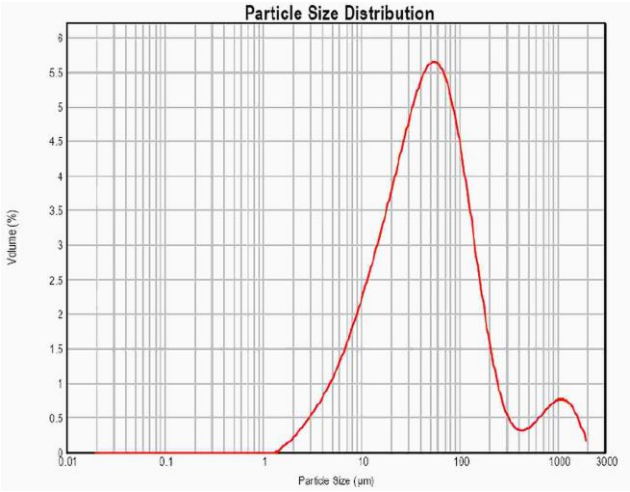

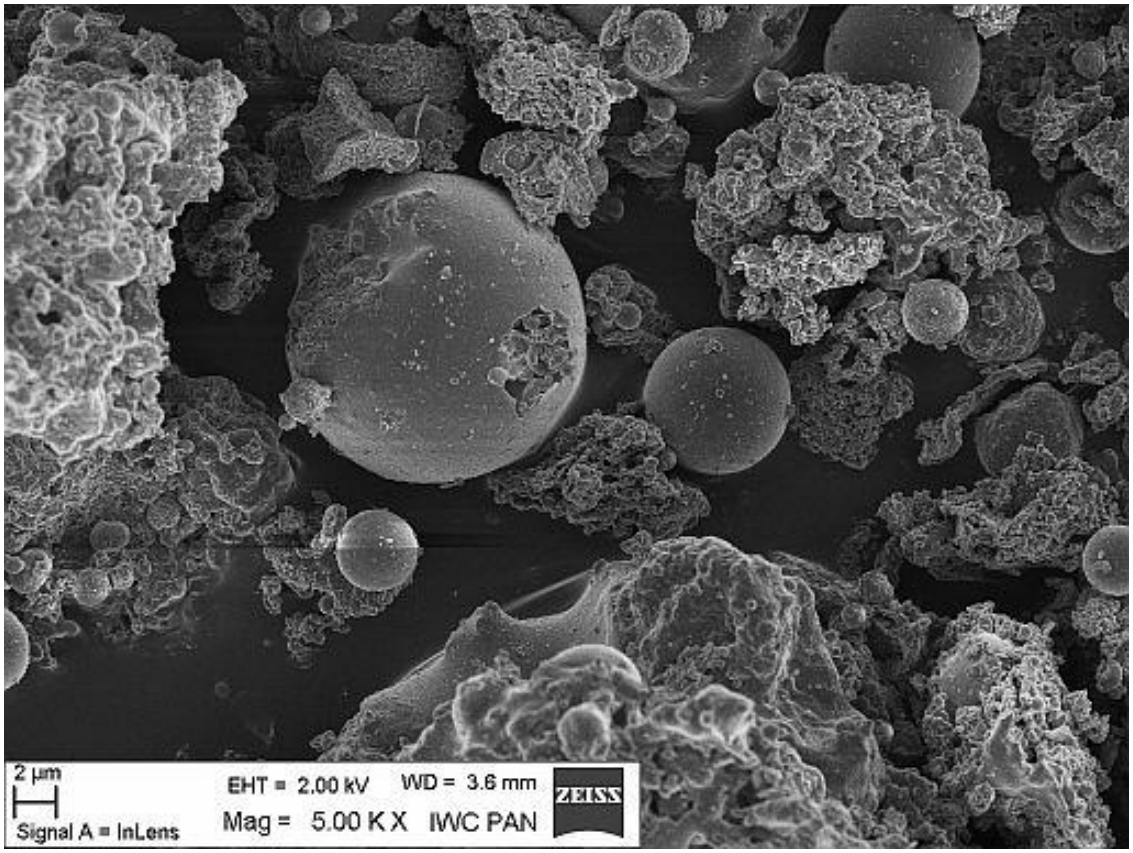

also:
XRD, DTA/TG/DTG,
SEM-EDS, chemical

Development of new blended cements

Types and principal properties of blended cements
(reduced clinker content and properties for high range applications)

Cement type	Additives content, %	Specific density, g/cm^3	Specific surface Blaine, cm^2/g	Water demand, %	Soundness Le Chatelier, mm	Compressive strength, MPa	
						2 days	28 days
CEM I (Portland)	0	3.10	3830	26.5	0	27.5	56.3
CEM II/A-W	15	3.05	3840	29.0	0	24.1	52.5
CEM II/B-W	30	2.98	3760	31.6	0	16.4	46.8
CEM II/B-M (V-W)	15+15	2.93	3750	30.4	0	18.7	44.9
CEM II/B-M (S-W)	15+15	3.03	3720	29.0	0	19.4	54.8
“CEM V/A (S-W)”	25+25	2.97	3810	29.8	0	11.7	40.3

W – high calcium fly ash (lignite)
V – siliceous fly ash (hard coal)
S – ground granulated blastfurnace slag

Frost -deicer scaling resistance of concrete: blended cements and processed HCFA

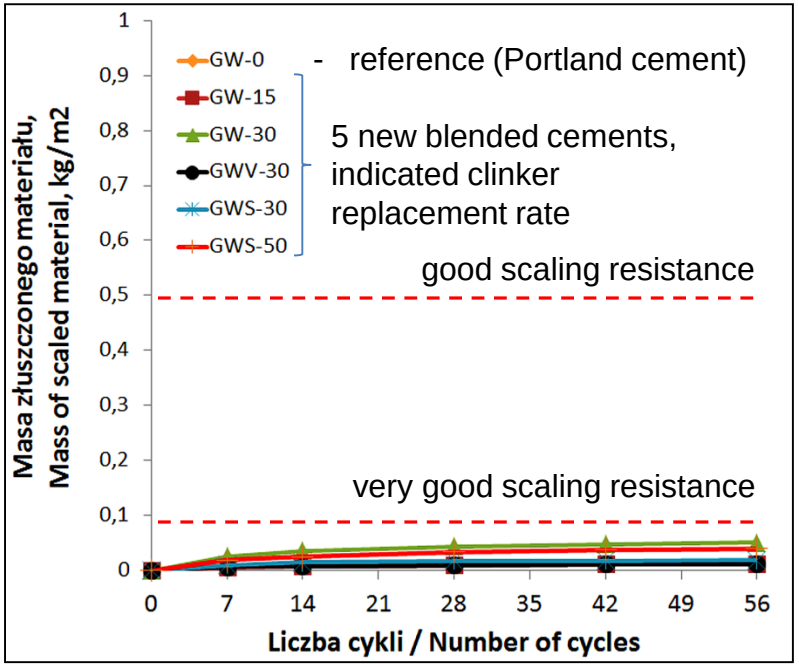

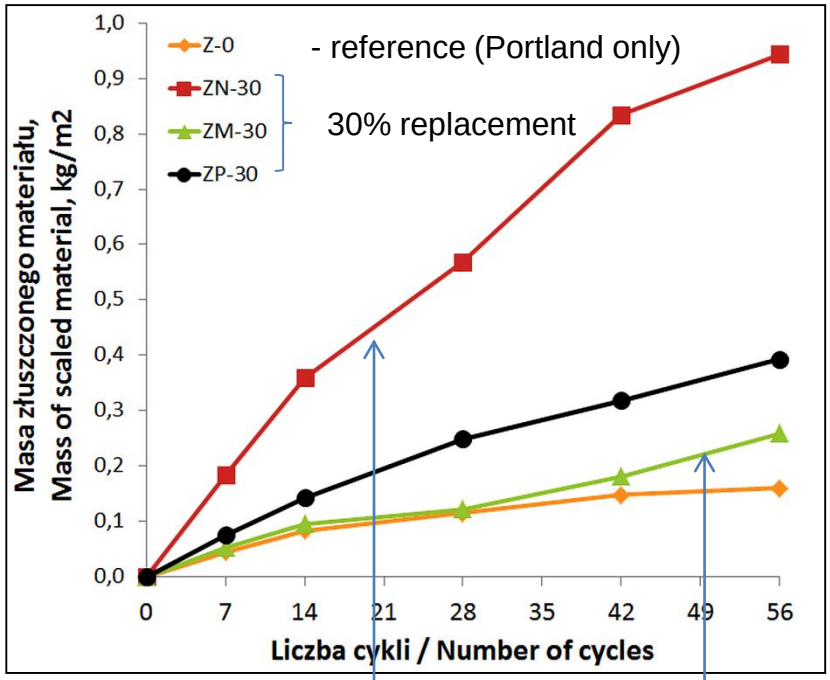

New blended cements are found to provide much greater stability of air void system in concrete

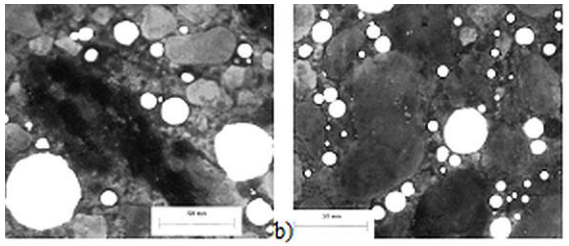

α=20,9mm^{-1} α=36,9mm^{-1}
specific surface of air voids

Quantitative characterization of concrete micostructure -air void system

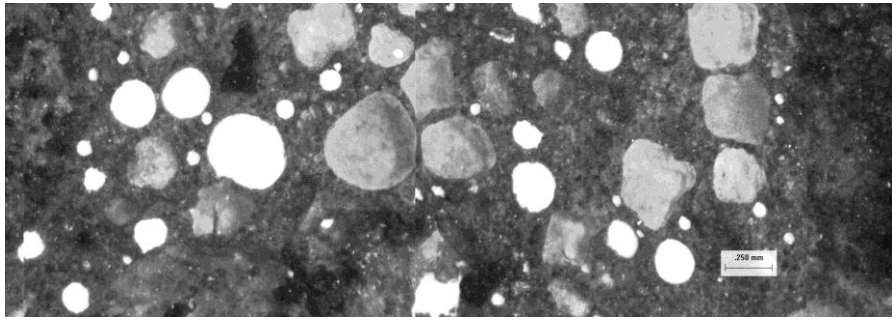

Air voids (white) in a polished section of concrete with CFBC fly ash (optical microscopy with digital image analysis)

Spacing factor of air voids system versus the content of CFBC fly ash

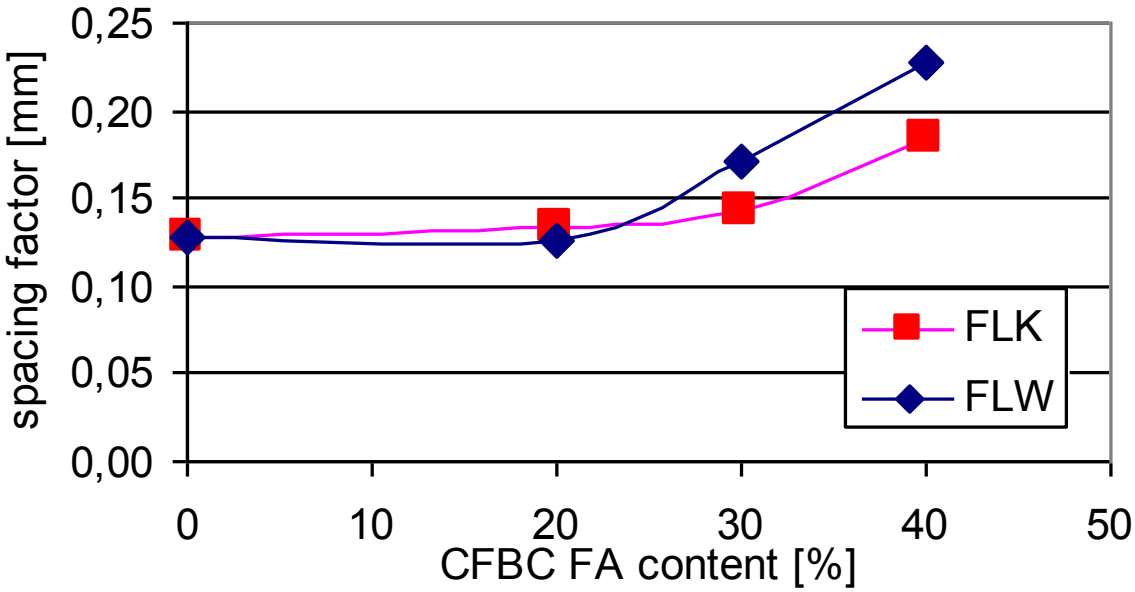

Air voids and scaling of slag blended cement concrete

Highly increased frost-salt scaling

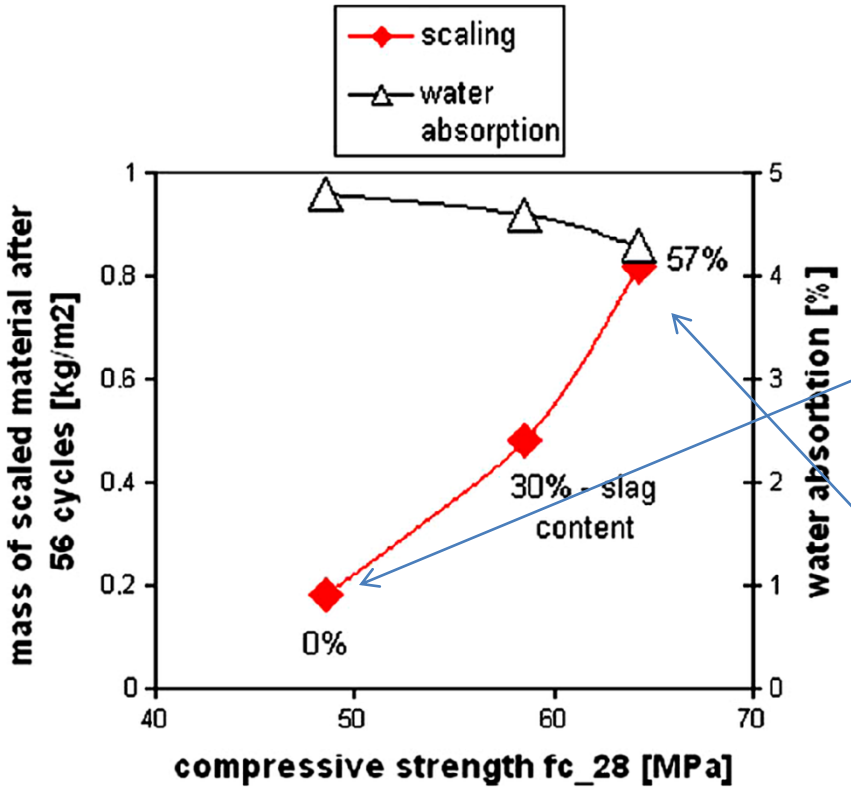

Air void size distribution in concrete

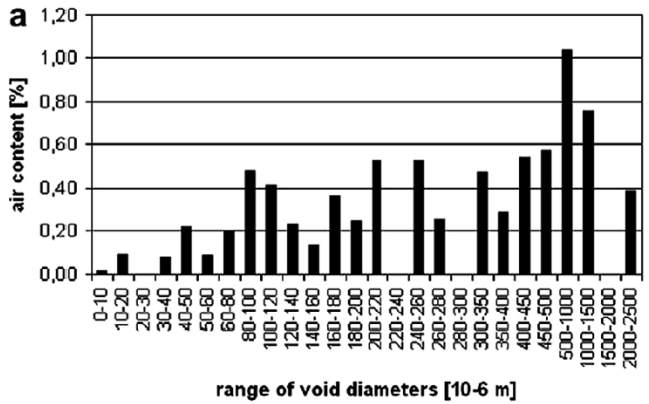

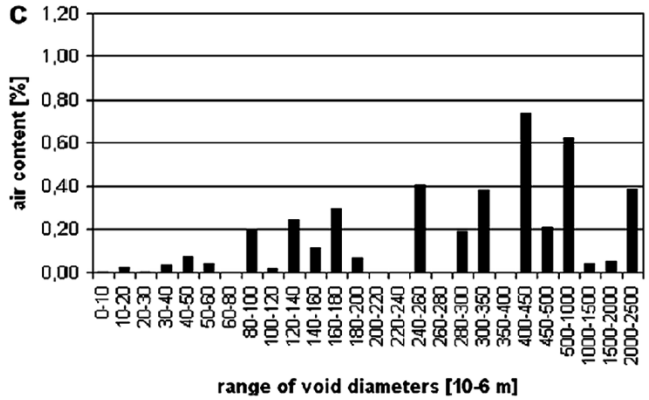

Inhomogeneities of air void system

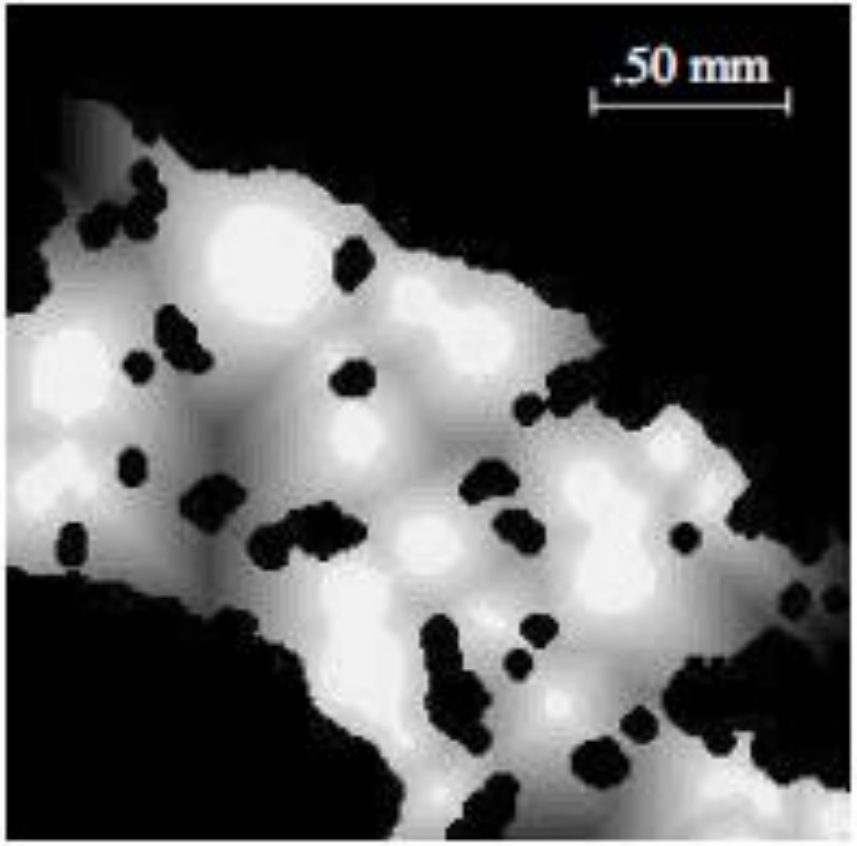

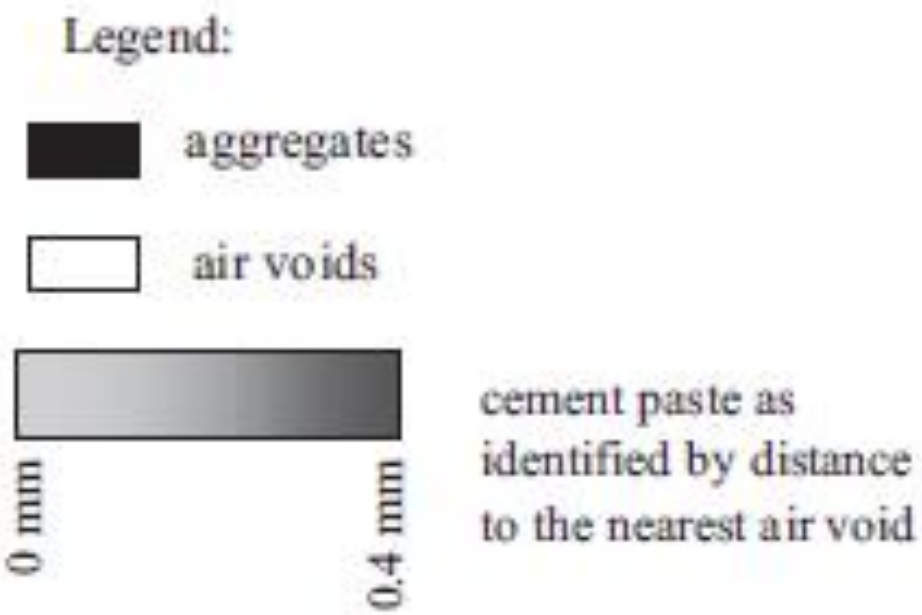

The area fraction of the cement paste within a selected distance from the periphery of air voids can be calculated.

Quantitative characterization of carbonation process

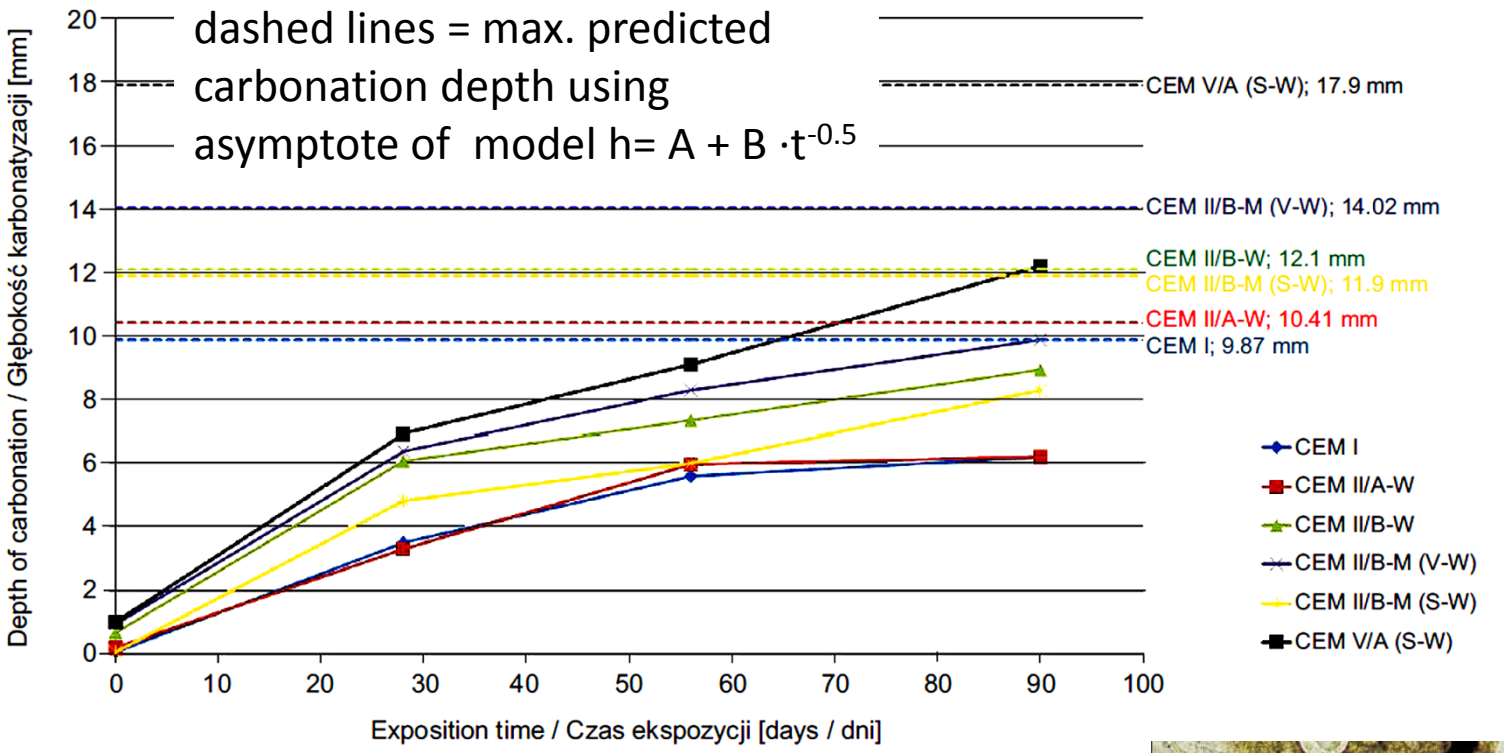

Thin section image in polarized light to analyse the carbonation front

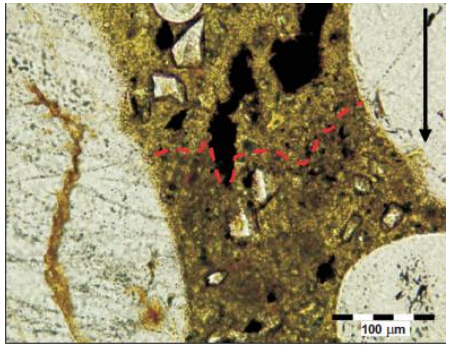

Processing of image of cracks on impregnated flat sections

segmentation filtering
operations shape analysis

skeletonization

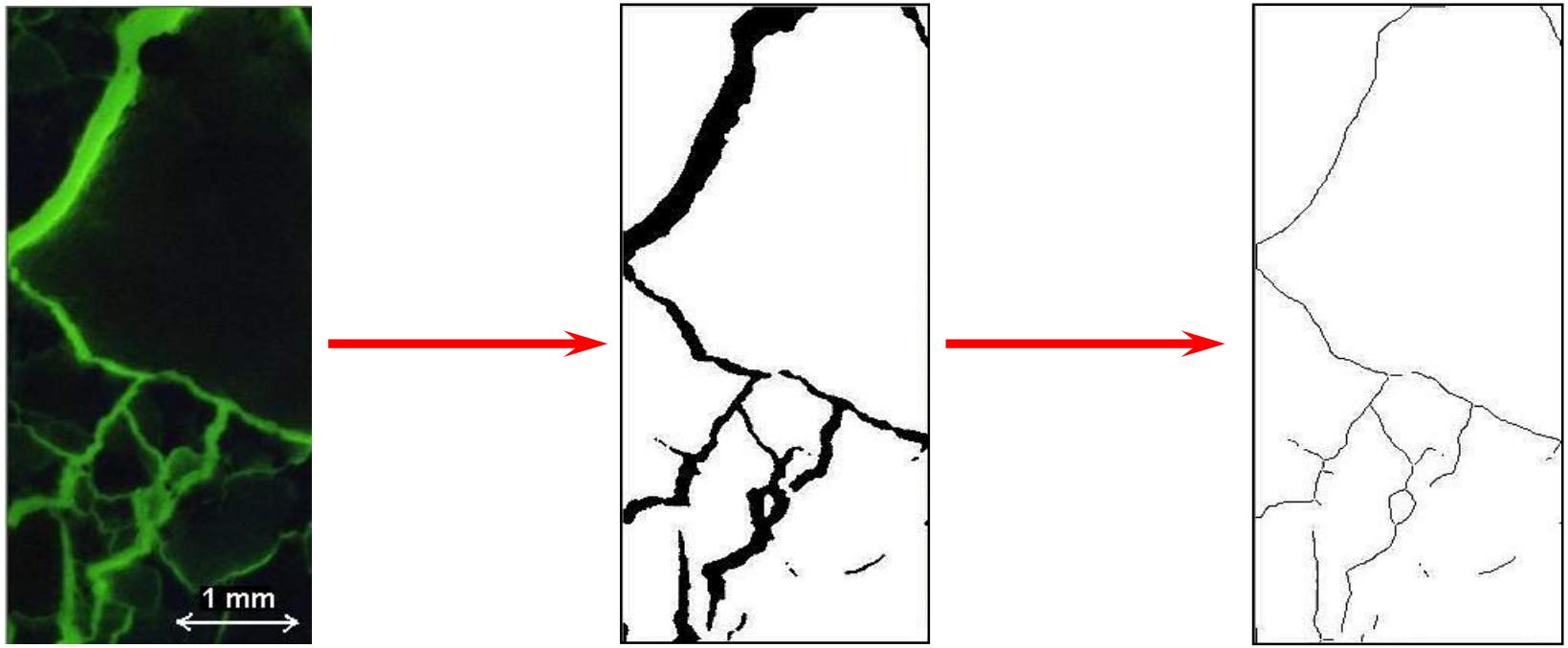

Quantitative parameters of crack system

- Crack density =total dendritic length of cracks per image area
- Degree of crack orientation—shown by means of “rose of intercepts”
- Distribution of crack width—shown as percentage object fraction in the given range of crack width

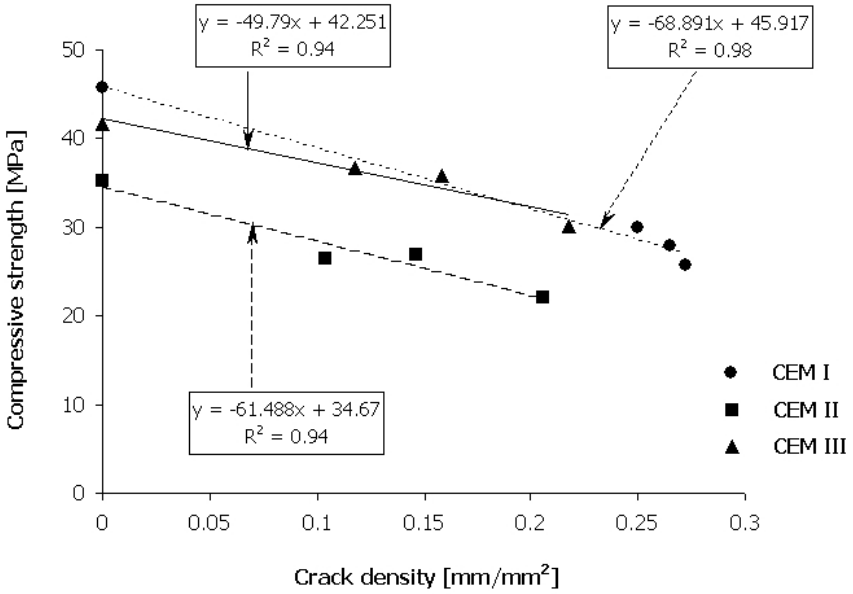

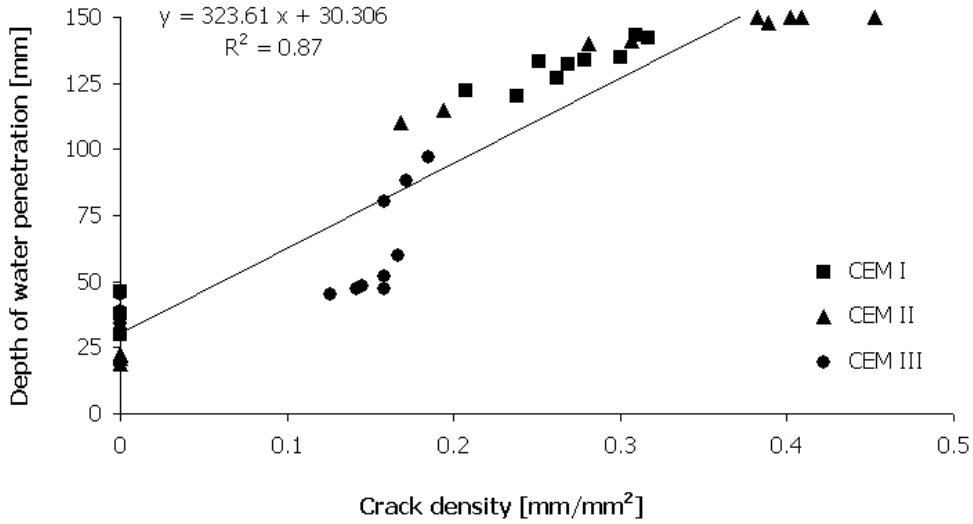

Crack density in concrete damaged due to early freezing

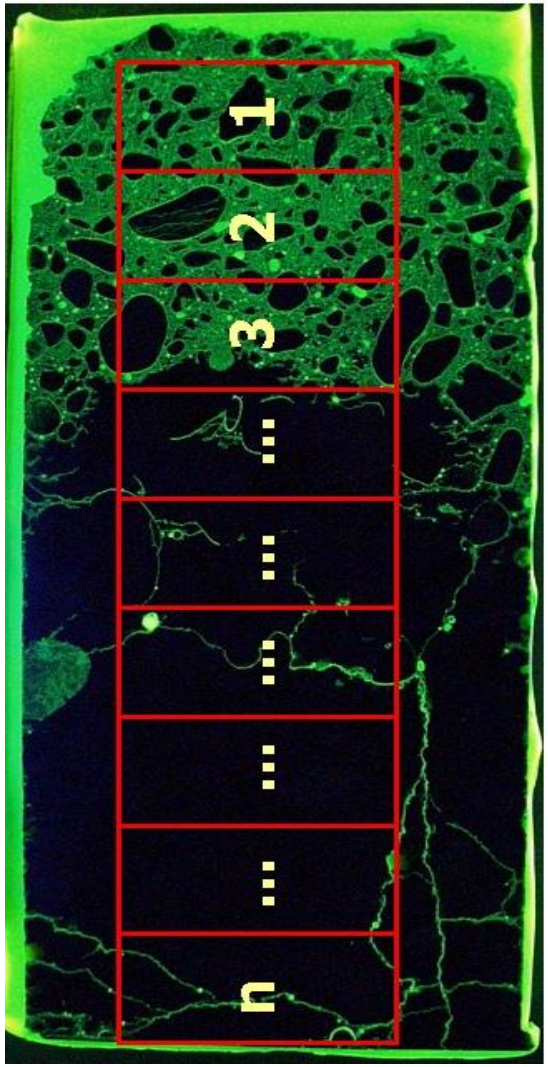

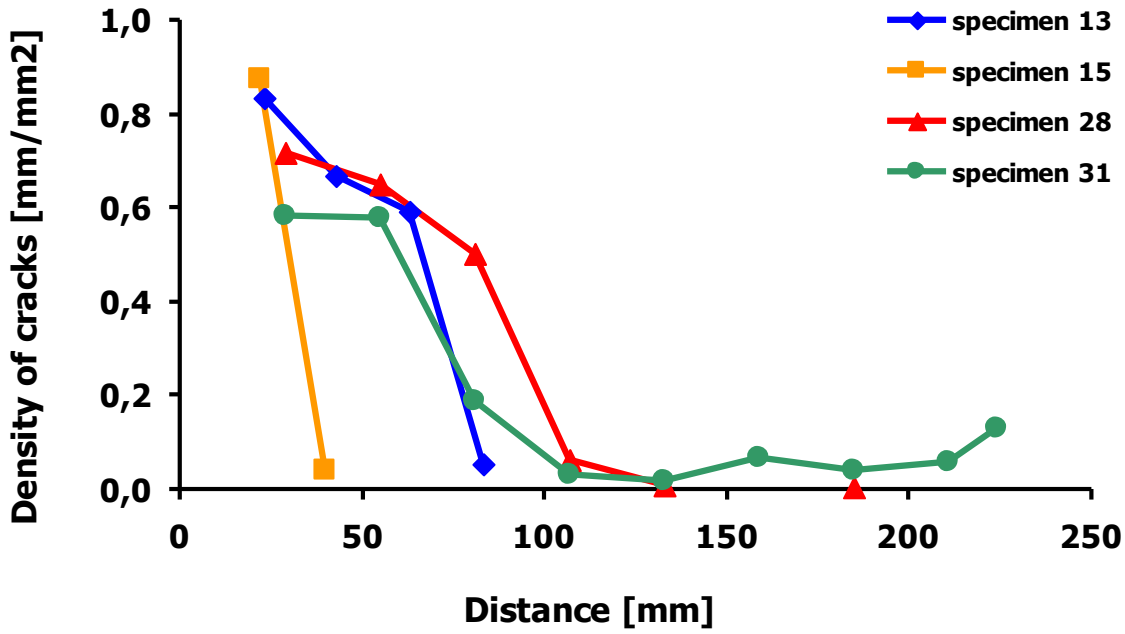

Almost nondestructive diagnostics of concrete durability

structure

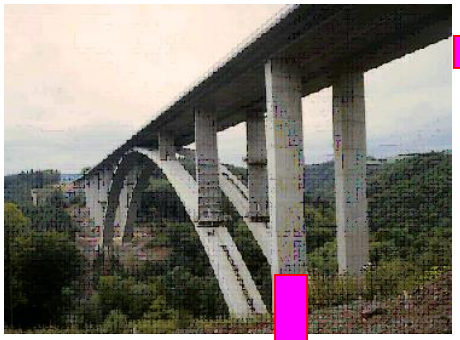

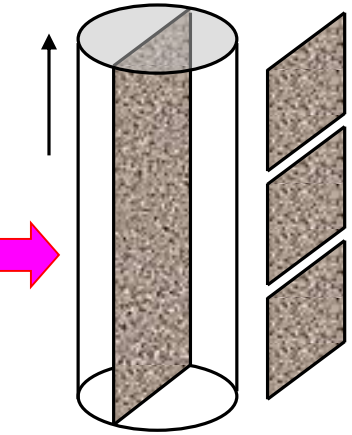

core specimen

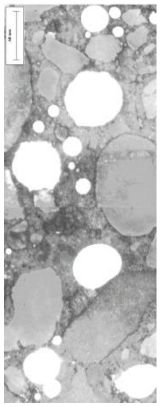

section

DSI

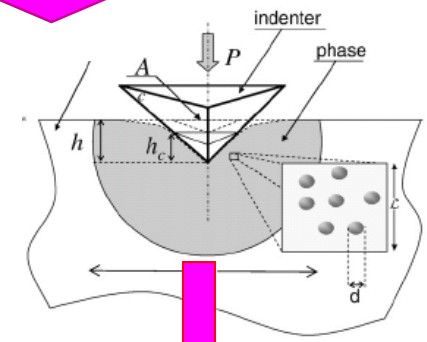

Permeability testing

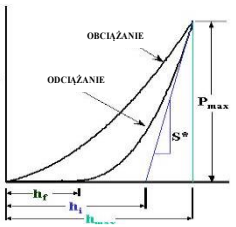

HV (matrix)
E (matrix)
EA

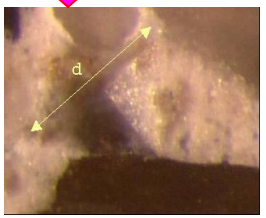

component identification

Classification of durability in aggressive environment

Local characterization of matrix by microindentation

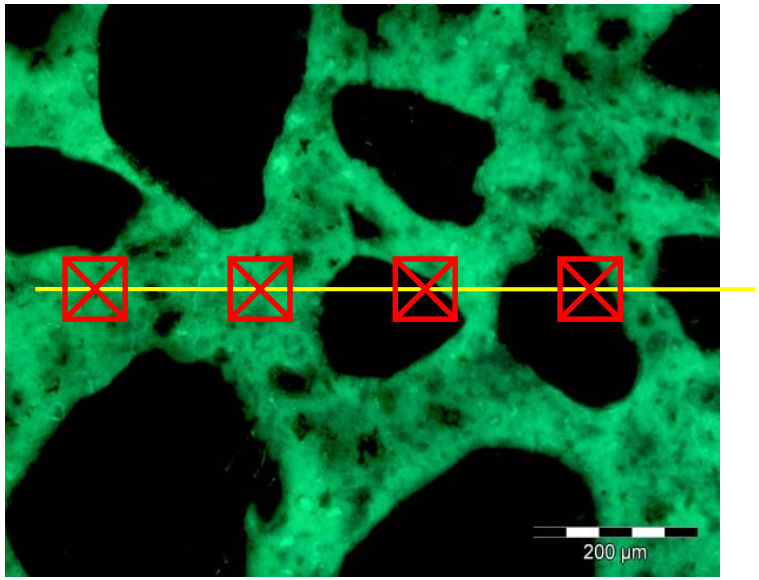

Continuous measurement of load, penetration depth and acoustic emission

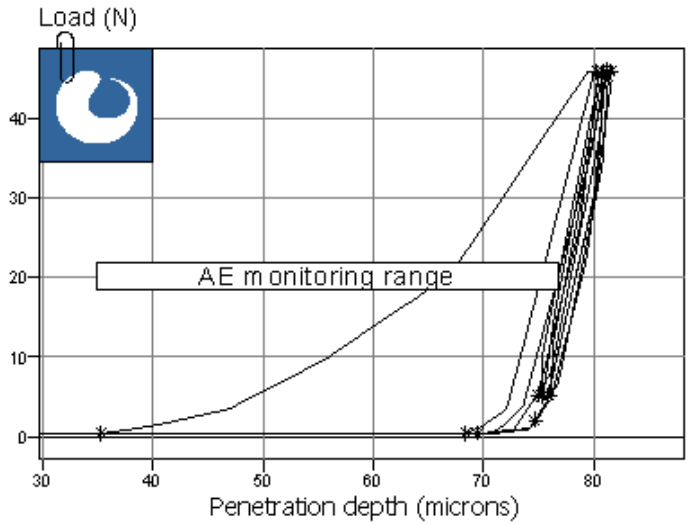

Relationship between frost-salt scaling resistance and paste microhardness

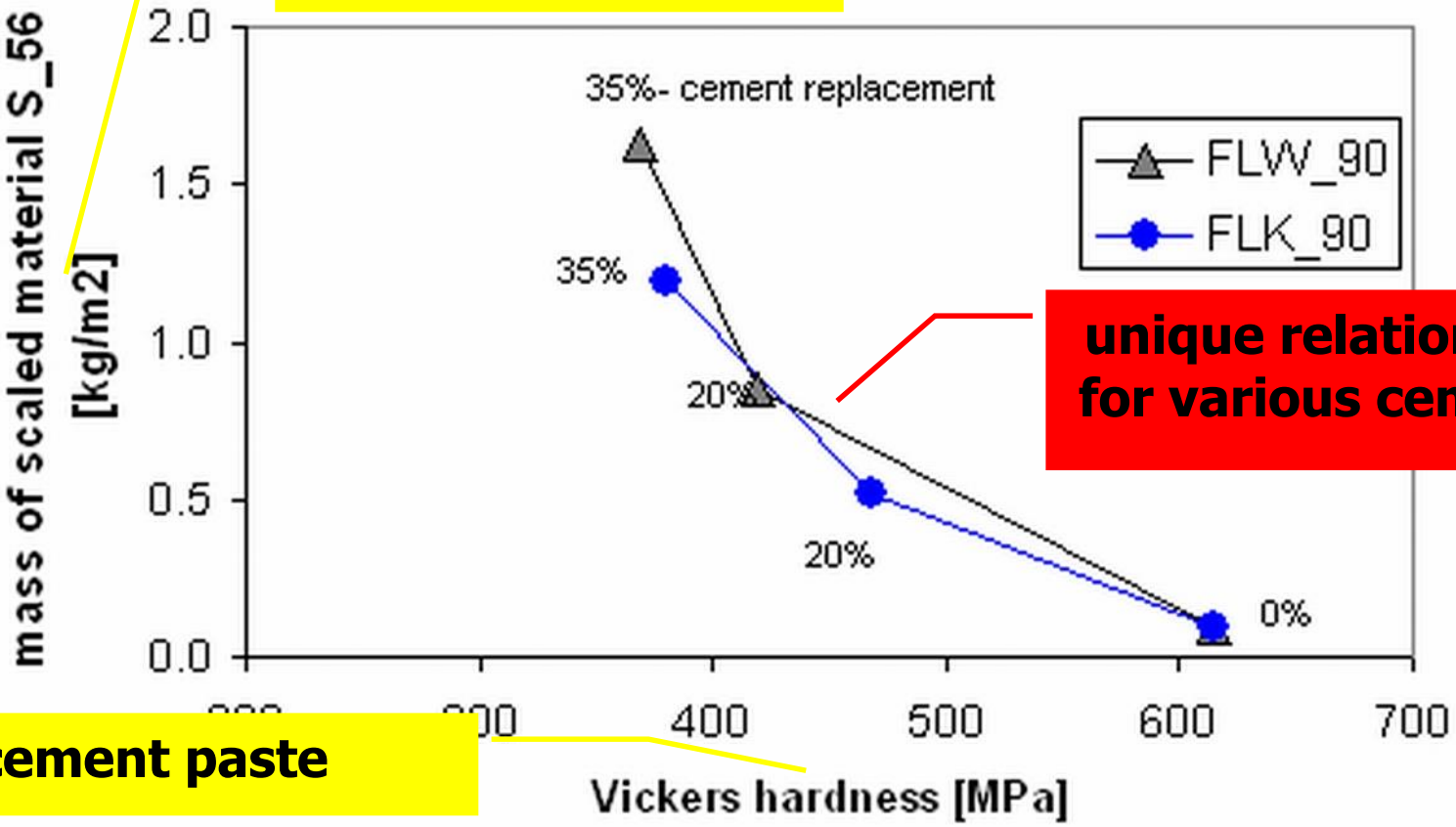

Identification of ‘low density’ and ‘high density’ areas using microindentation

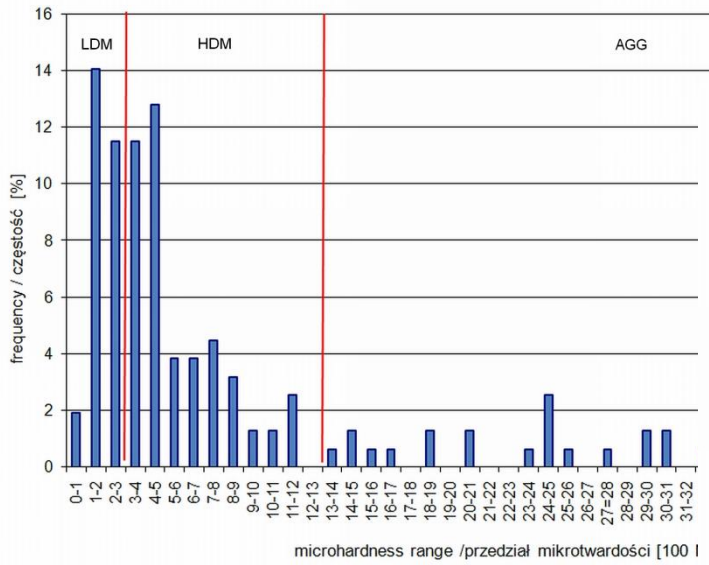

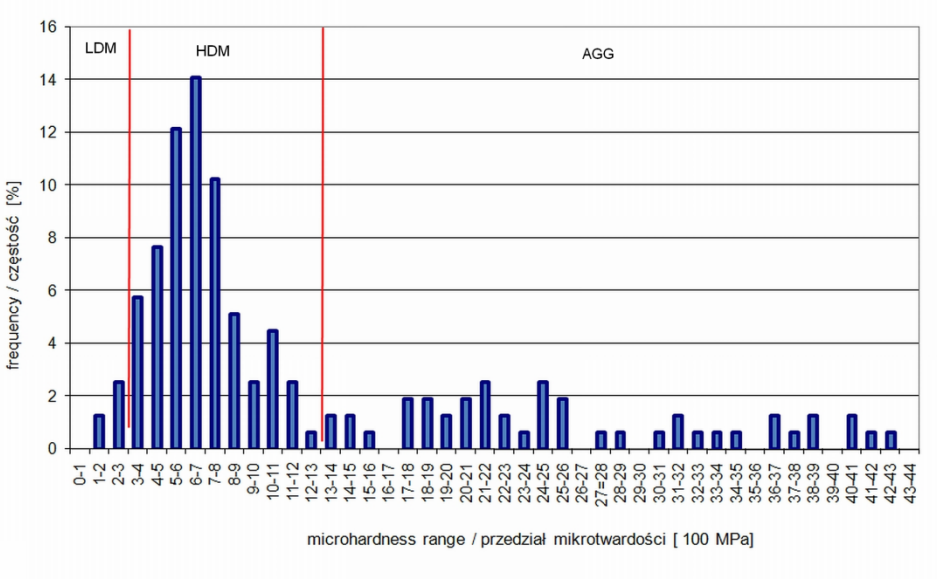

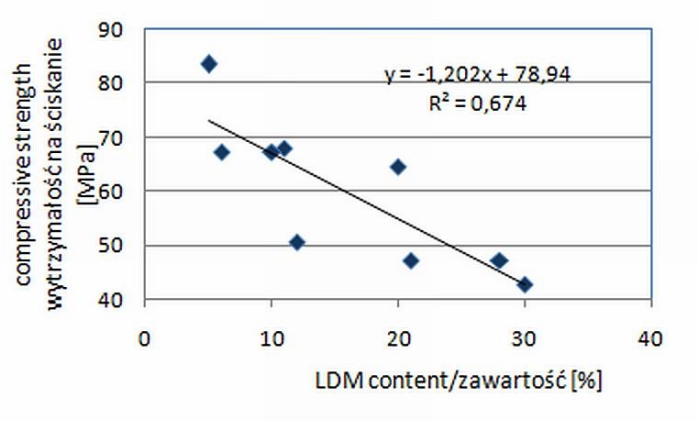

Relationship between the LDM content and the compressive strength of concrete

Long-term toughness of glass fibre concrete

Improvement of long term toughness of GFRC in highly alcaline environment of cement paste at high humidity and increased temperature

Flexural performance before and after ageing

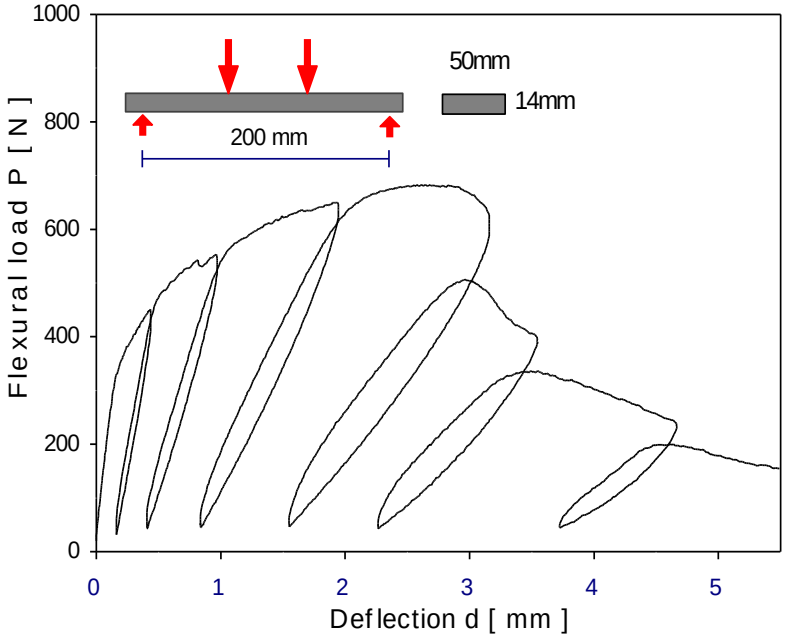

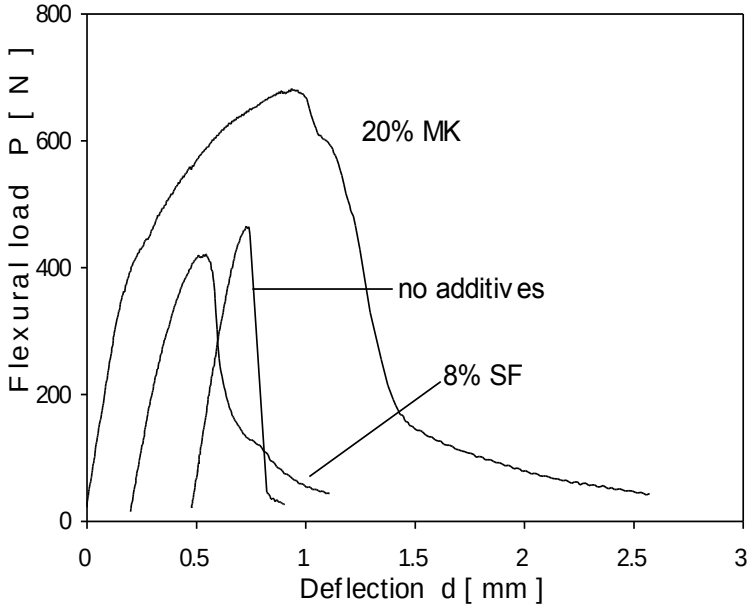

Push-out and push back tests on single fibres

- 50 to 200 glass filaments in strand

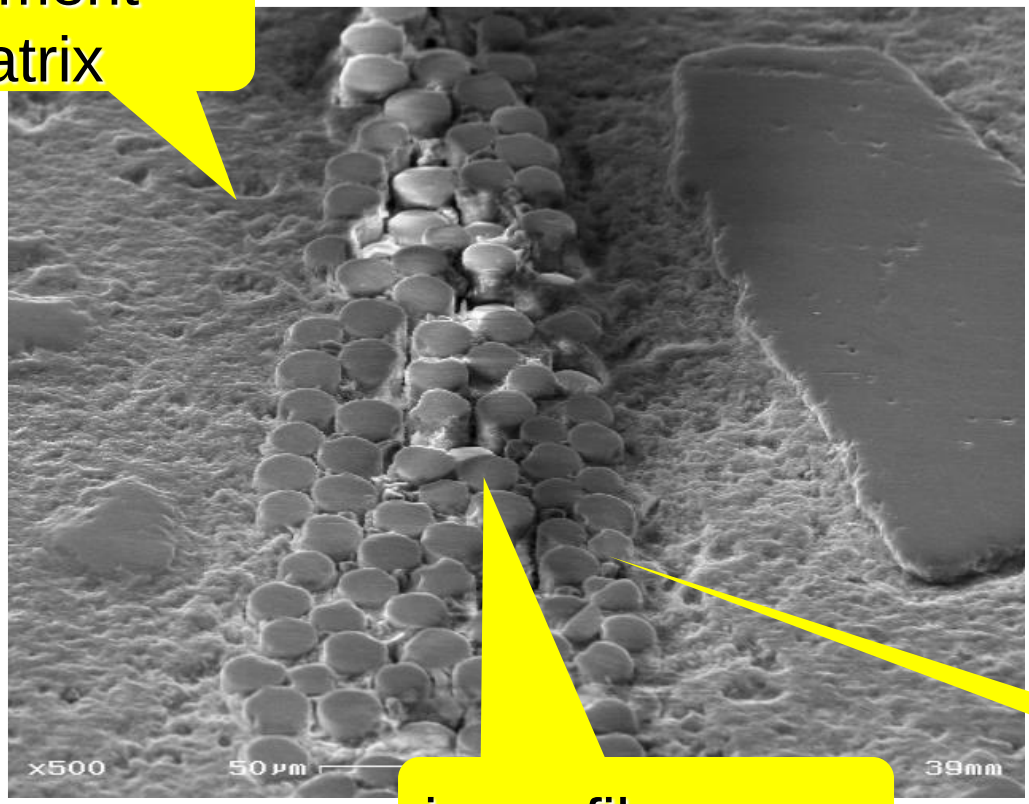

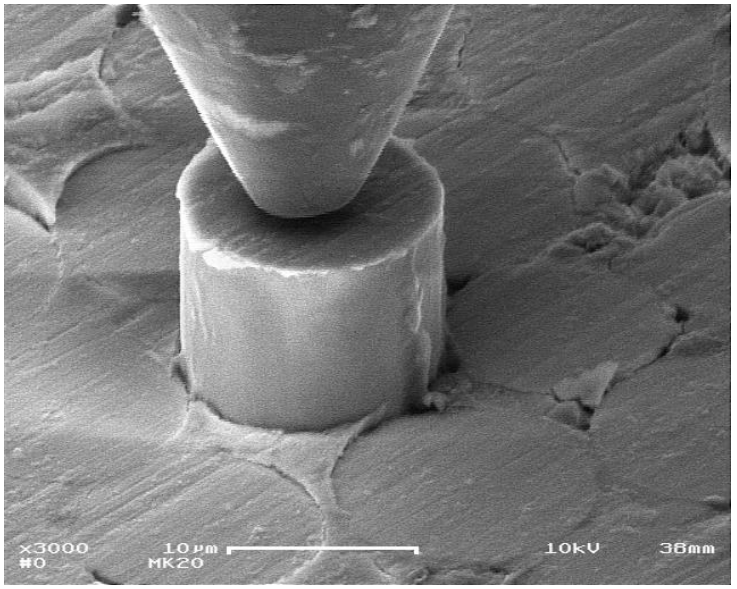

Fiber-cement interface characterization: push-out results

Matrix: cement 70%+metakaolin 30%
quartz sand 0.25mm

inner fibres

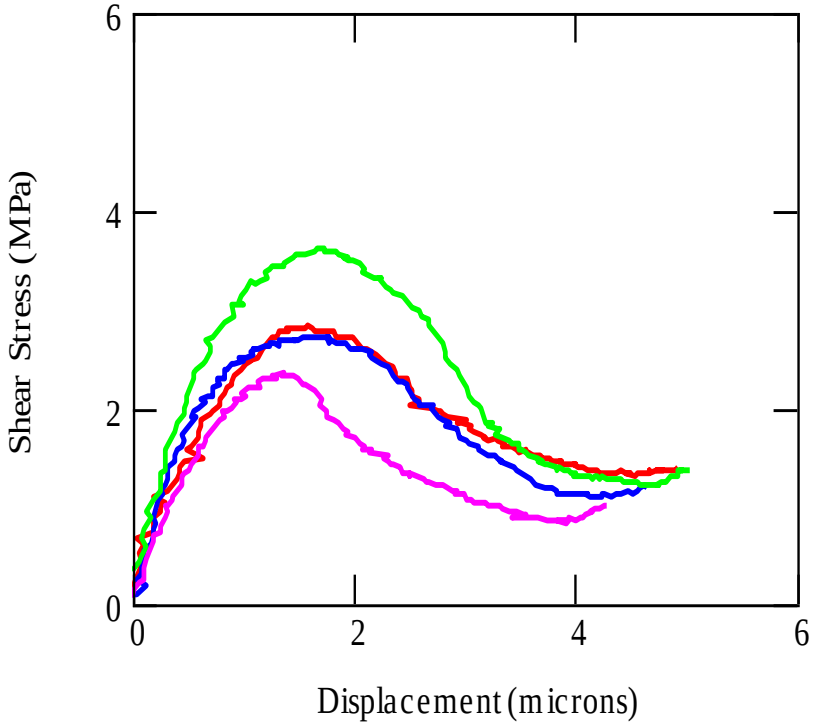

outer fibres

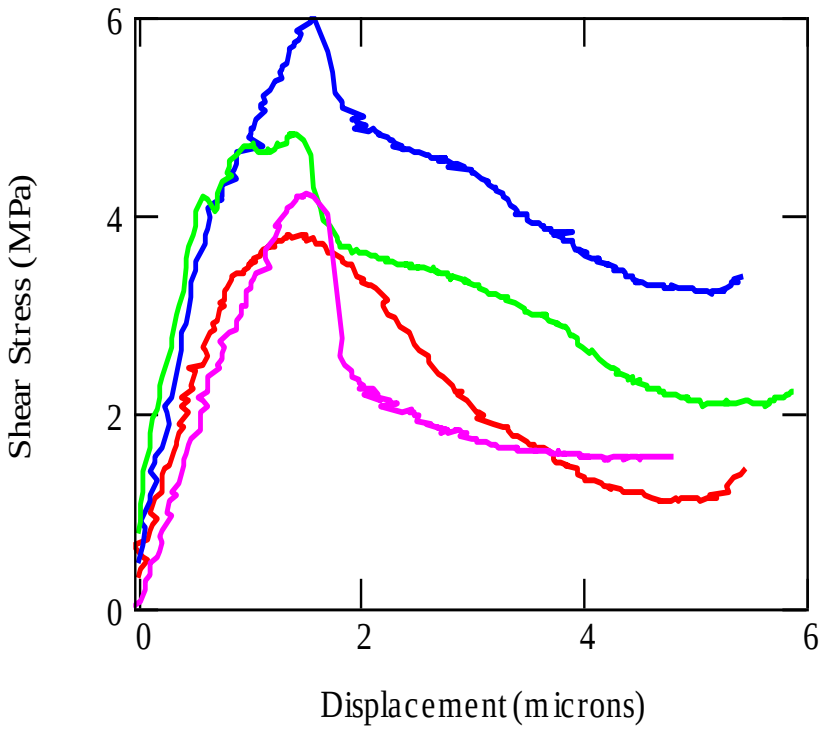

Development of fibre-matrix interface model

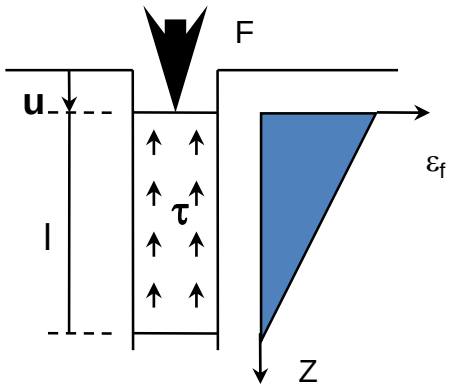

$$u = \frac{F^2}{4\pi^2 R^3 \tau E_f} - \frac{2\,\Gamma_i}{\tau}$$

$2\,\Gamma_i$ - fracture surface energy per unit area of interface

τ - constant shear stress at the interface

Debonding energy Γ_i

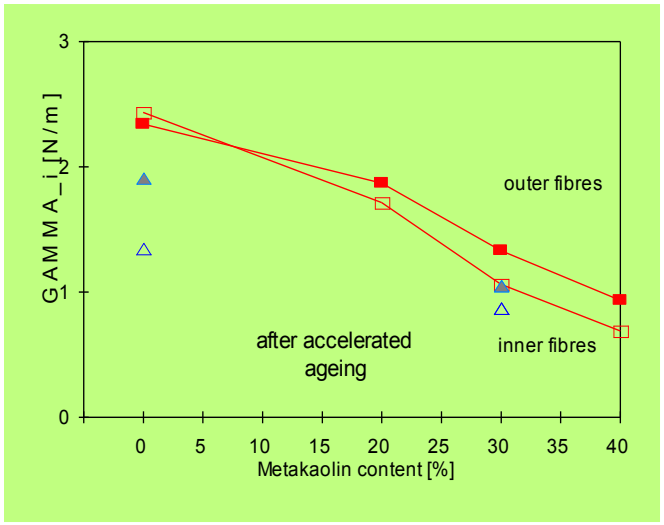

Friction stress τ

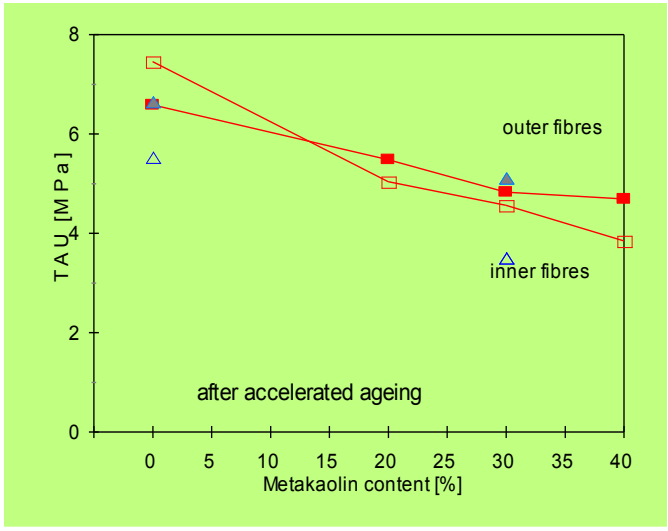

Bond strength of single filaments after ageing → fracture mechanisms

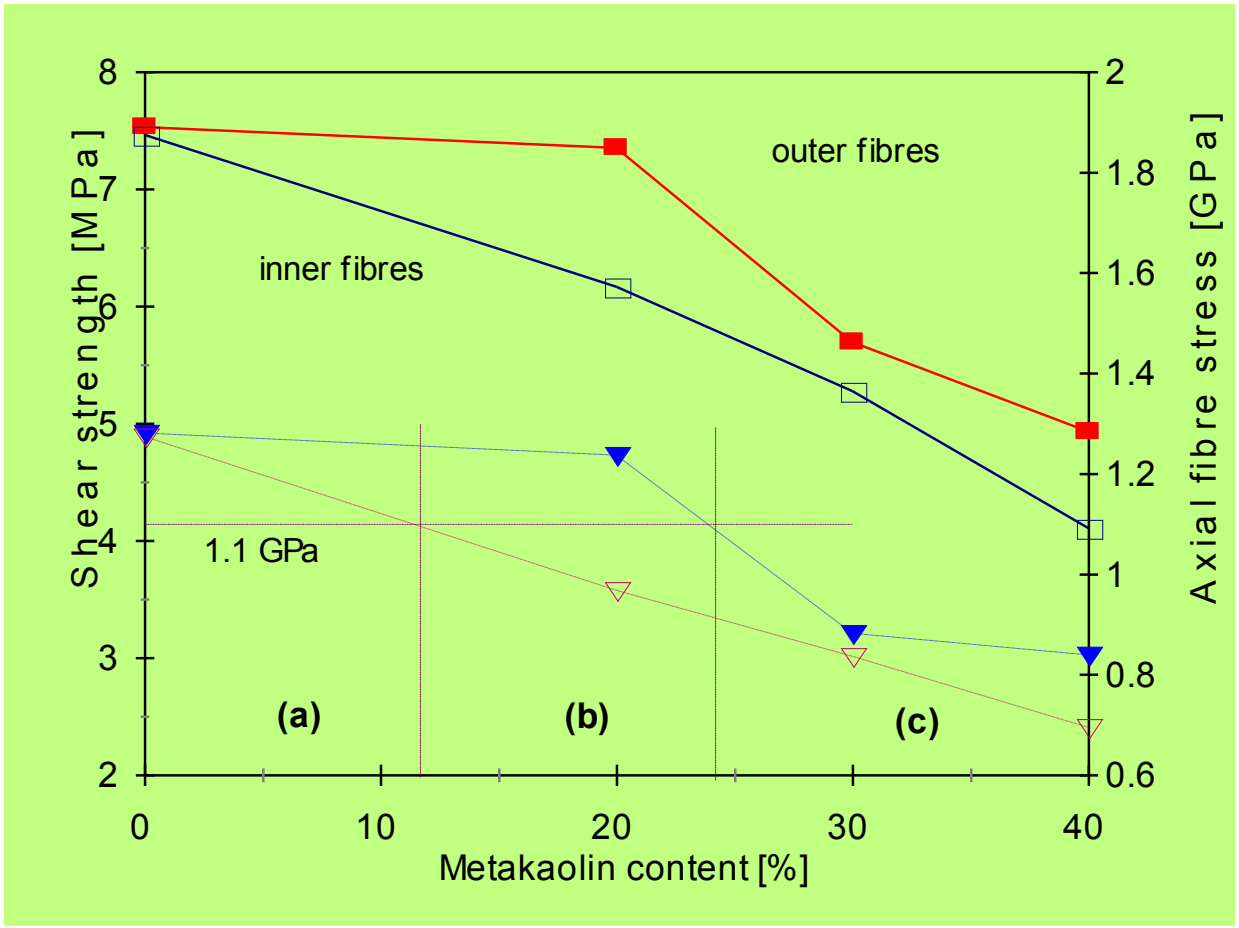

Fracture mechanisms :

a) fibre fracture

b) telescopic fracture of strand

c) fibre pull-out

Studies of thermal properties of hardening concrete

Heat transfer model

$$c\rho\frac{\partial T}{\partial t}-\frac{\partial}{\partial x}\left(k_x\frac{\partial T}{\partial x}\right)-\frac{\partial}{\partial y}\left(k_y\frac{\partial T}{\partial y}\right)-\frac{\partial}{\partial z}\left(k_z\frac{\partial T}{\partial z}\right)=Q$$

ρ – density, c – heat capacity, T – temperature, t – time,
x, y, z – spatial coordinates, Q – heat source function
k_x, k_y, k_z – thermal conductivity in direction x, y, z respectively

Method based on the solution of **INVERSE HEAT TRANSFER PROBLEM**
→ tool for evaluation of thermal performance of new concrete mixtures containing nonconventional mineral components

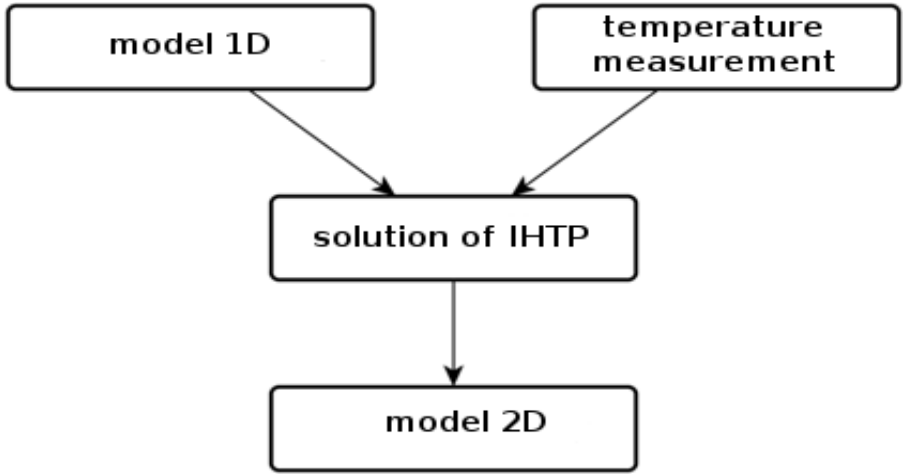

1 D heat transfer during hardening

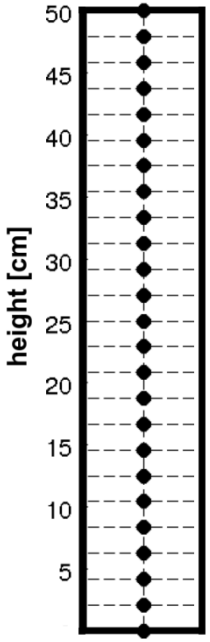

FDM - finite-difference method in spatial domain, Dirichlet boundary conditions

Temperature monitoring during 72 hours

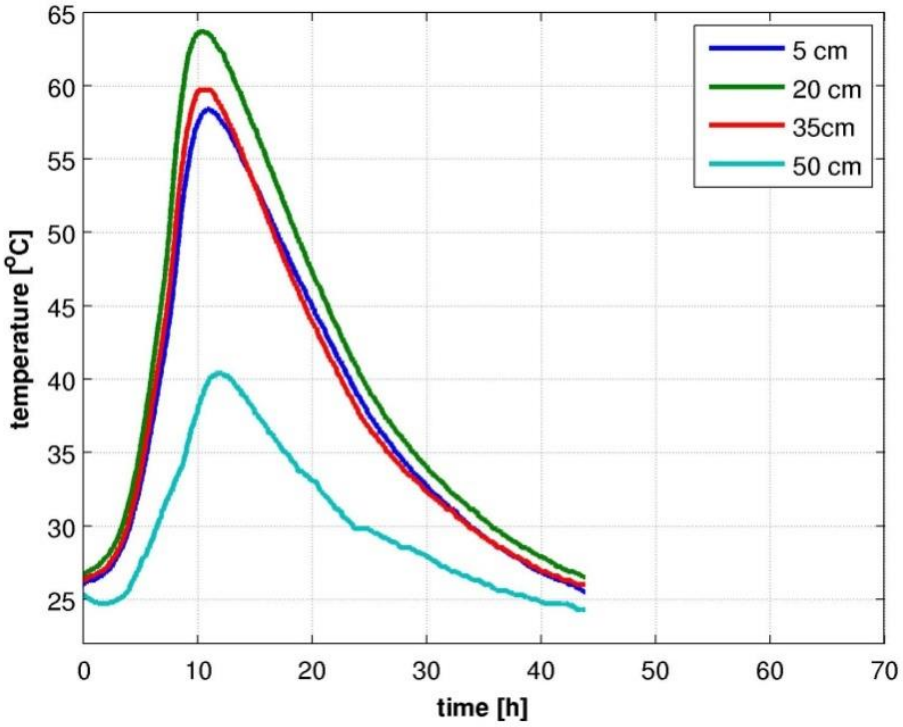

Results of inverse heat transfer analysis

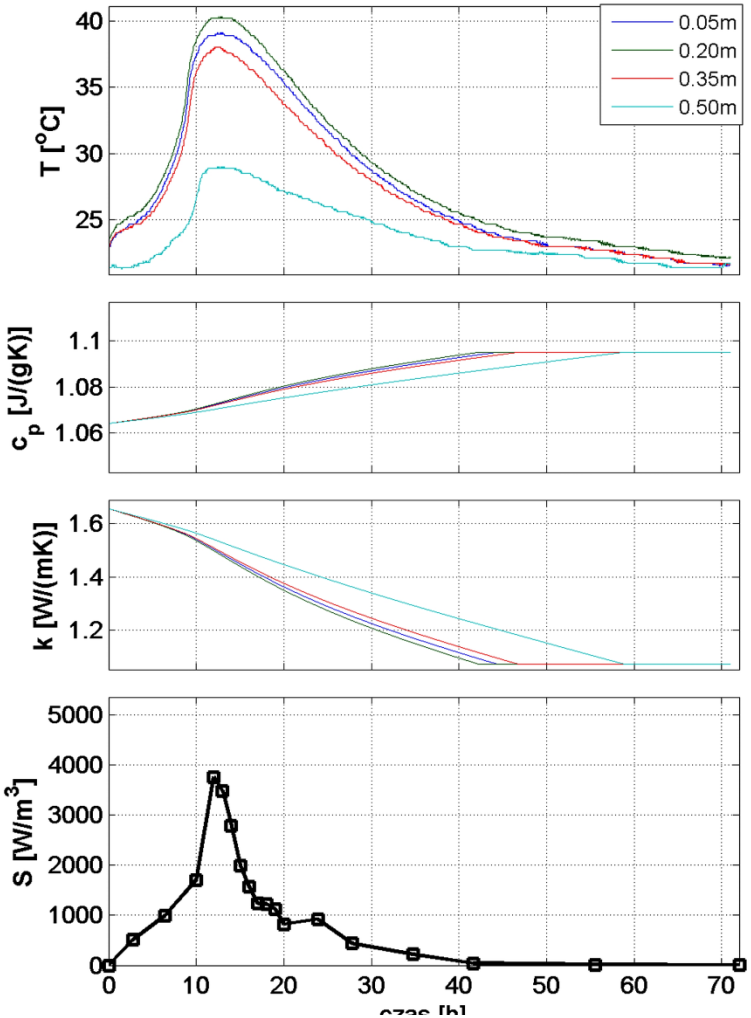

Measured temperature distribution in time in hardening concrete (1D element)

Calculated:
-specific heat,
-coefficient of thermal conductivity and
-heat of hardening
in time for concrete mix containing 30% of nonstandard SCM

Temperature predictions and actual measurements in large concrete blocks

Temperature distribution in cross section at 25 h

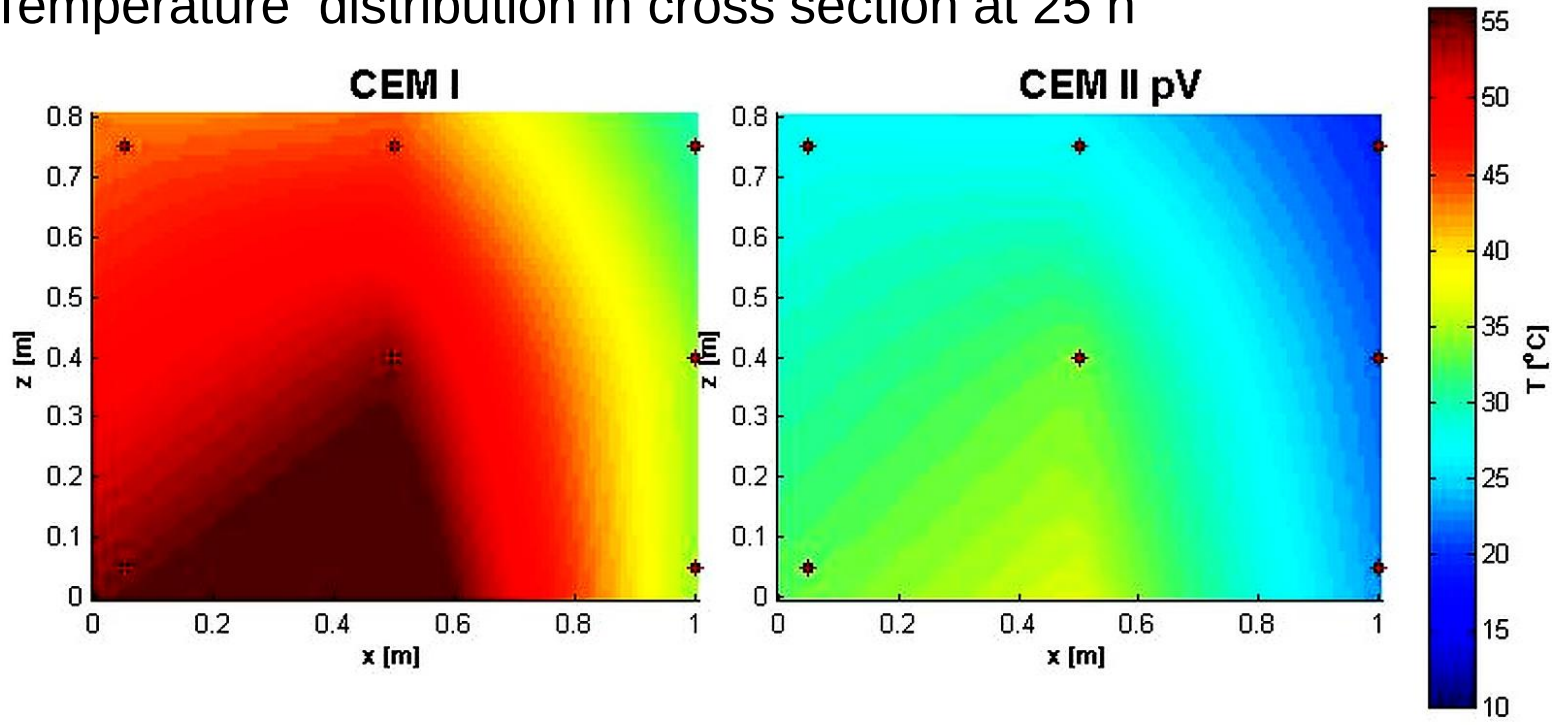

Left: Portland cement
Right: 30% replacement by HCFA

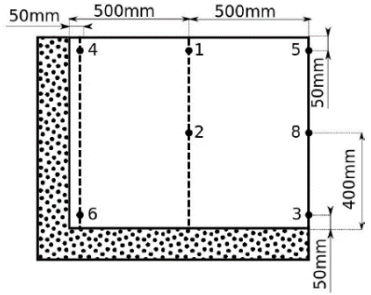

Block size and temperature sensor location

Application of soft computing methods to aid in prediction of concrete durability

Objective

to develop rules for automatic categorization of concrete quality using machine learning techniques,
in particular:
- the rules for categorization of resistance of concrete to chloride migration and resistance to frost-salt aggression
- prediction of mechanical properties of recycled aggregate concrete

Range of materials
concrete mixes containing new highly active mineral additives replacing Portland cement and developed new blended cements; recycled aggregate concrete

Database used for machine learning application

C1	pfT	pfK	W	A_fr	fc28	Resistance
360	0	0	162	2.1	55.0	Acceptable
306	0	54	162	1.8	56.2	Acceptable
252	0	108	162	1.3	51.6	Good
306	54	0	162	1.6	60.3	Good
252	108	0	162	1.6	58.7	Good
380	0	0	171	6.2	46.3	Acceptable
323	0	57	171	6.8	47.2	Good
266	0	114	171	5.8	46.8	Good
323	57	0	171	6.6	45.3	Acceptable
266	114	0	171	6.2	46.3	Acceptable
406	0					
290	73					
217	14					
323	0					
244	0					

The database structure:
6 numerical attributes,
1 nominal attribute

C1 – content of cement, [kg/m3],
pfT, pfK – content of CFBC fly ash from brown and hard coal combustion, [kg/m3],
W – content of water, [kg/m3],
A_fr – air content in fresh mix, [%],
fc28 – compressive strength of concrete tested after 28 days, [MPa],
resistance – the resistance of concrete to chloride penetration (Acceptable, Good).

The rules based on J48* results

The decision tree generated by an J48 algorithm:

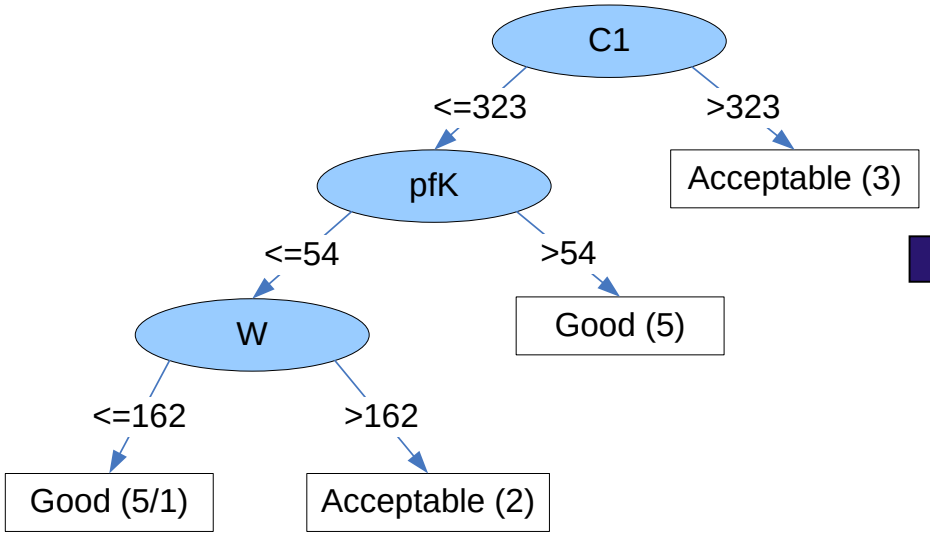

Corresponding rules

[Resistance = Good]
Rule 1
[C1<=323] and [pfK<=54] and [W<=162]

Rule 2
[C1<=323] and [pfK>54]

[Resistance = Acceptable]
Rule 1
[C1<=323] and [pfK<=54] and [W>162]

Rule 2
[C1>323]

* - algorithm J48 – the version of an algorithm C4.5 (invented by J. Quinlan); used ad a part of WEKA Workbench

Preventing leakage of the radioactive elements during the service life

Minimization of risk of cracking &leakage

At early ages:

- Due to thermal deformation
- Due to cold-joints, poor compaction

At service life:

- Due to thermal cycling
- ASR induced cracking
- Radiation induced cracking

An international panel of experts debated this question during the 123 Forum session at the Fall 2016 Concrete Convention and Exposition in Philadelphia, PA, on October 24, 2016. Eric Giannini and Tengfei Fu organized and moderated the session. The panelists included Kim Kurtis from the Georgia Institute of Technology, Yunping Xi from the University of Colorado, Michał Glinicki from the Polish Academy of Sciences, and John Provis from the University of Sheffield.

ASR prevention by selection of minerals

After accelerated expansion test- ASTM C1260

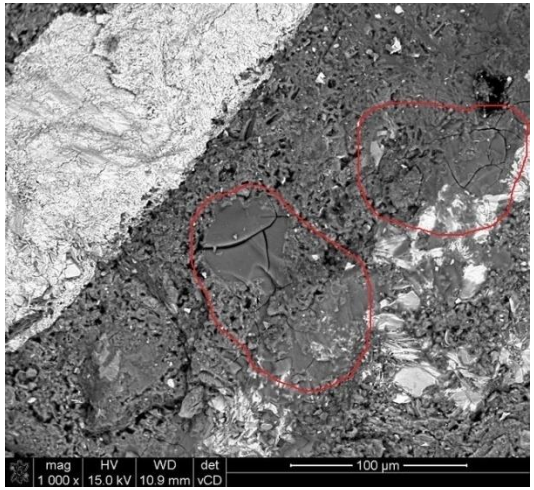

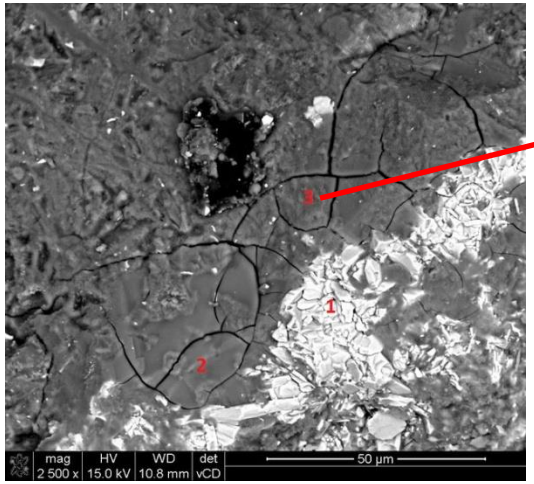

Hematite aggregate

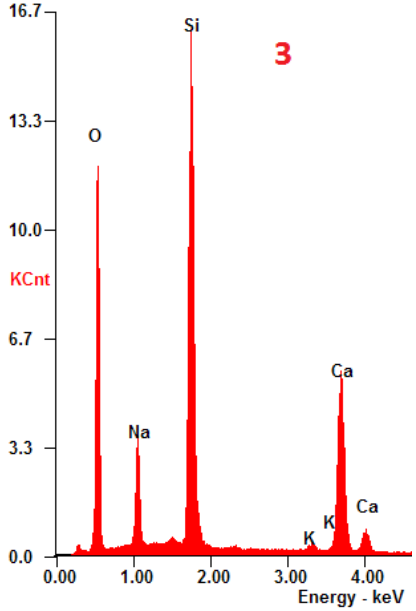

ASR gel

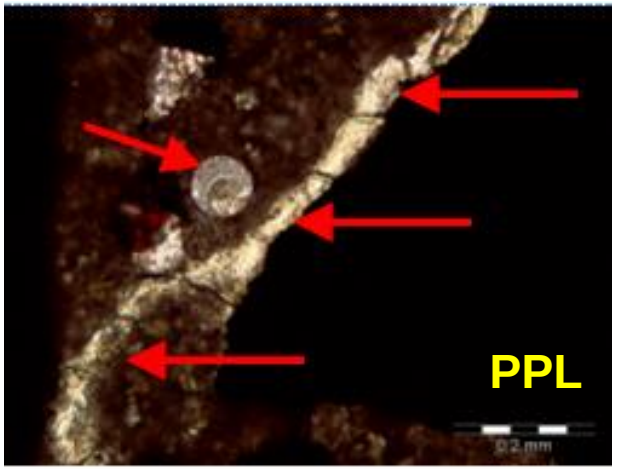

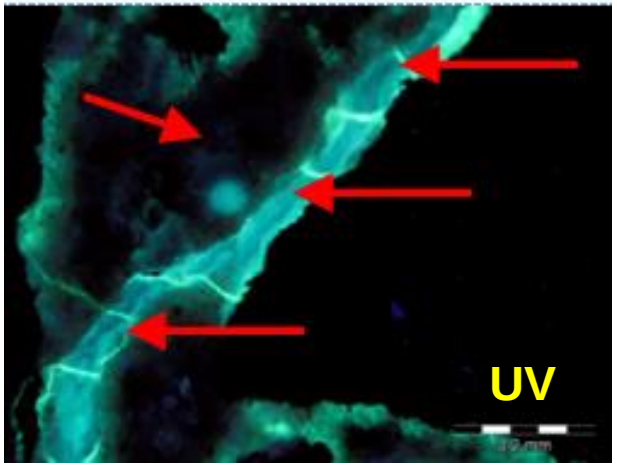

Early age thermal cracking prevention

More detailed characterization of thermal properties of hardening concrete by experimental-numerical approach

1. Unidirectional heat transfer test during 72 hours of hardening

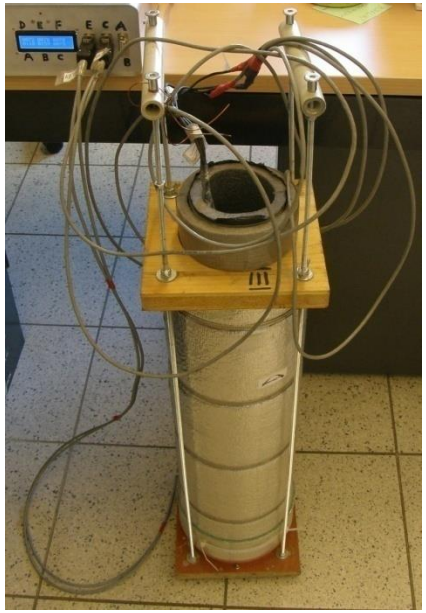

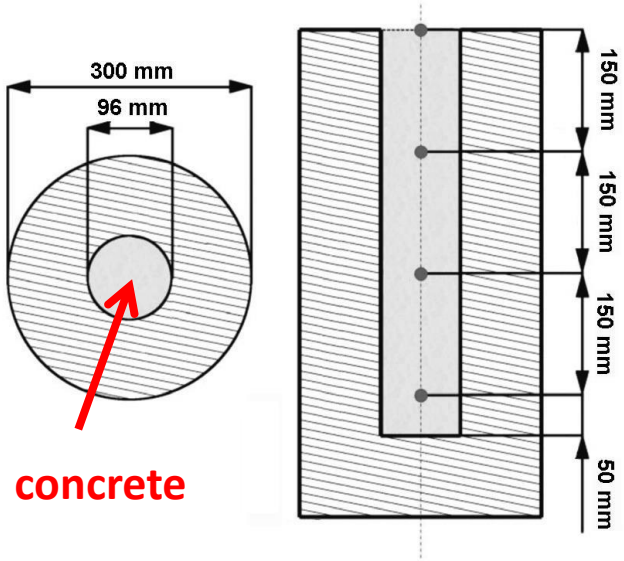

Early age thermal cracking prevention

2. Numerical solution of inverse problem of heat transfer

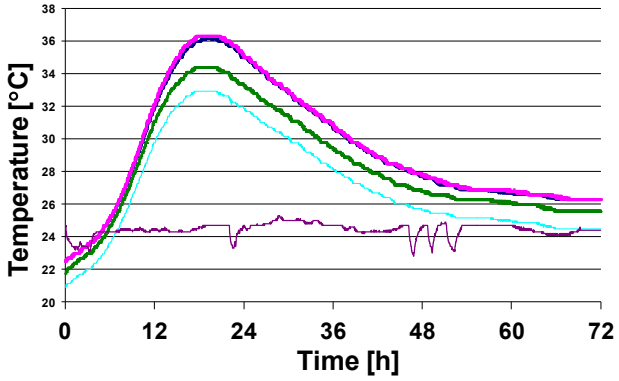

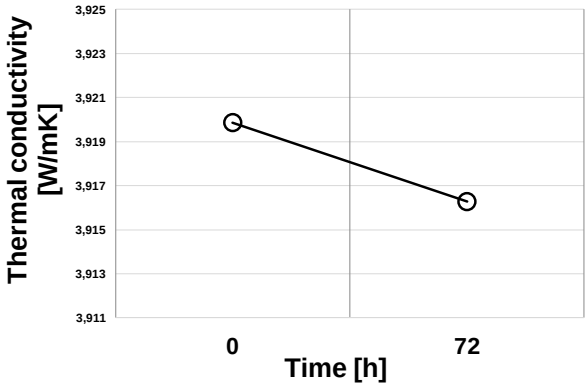

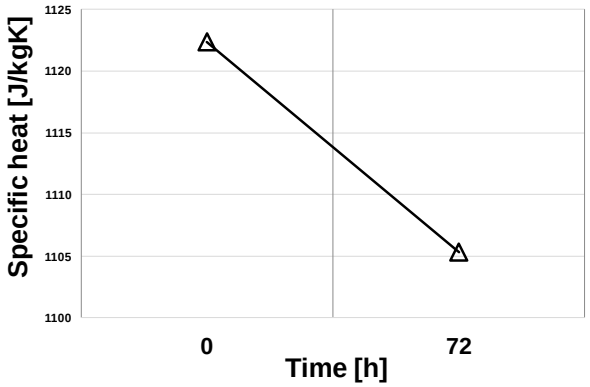

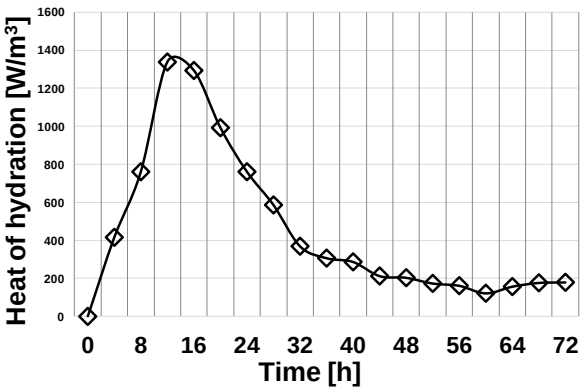

Early age thermal cracking prevention

3. Validation: large scale test and numerical simulation of heat flow in 3D

Selection of cements: CEM I, CEM II B-S, CEM III/A as per European standard EN 197-1 with special properties LH, NA

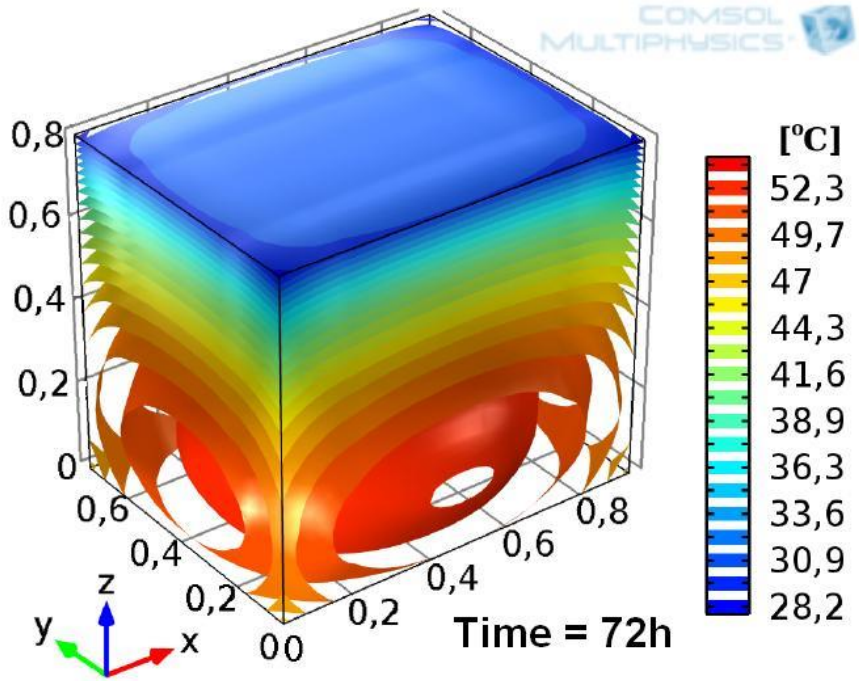

Self-compacting heawyweight concrete

and the formwork pressure

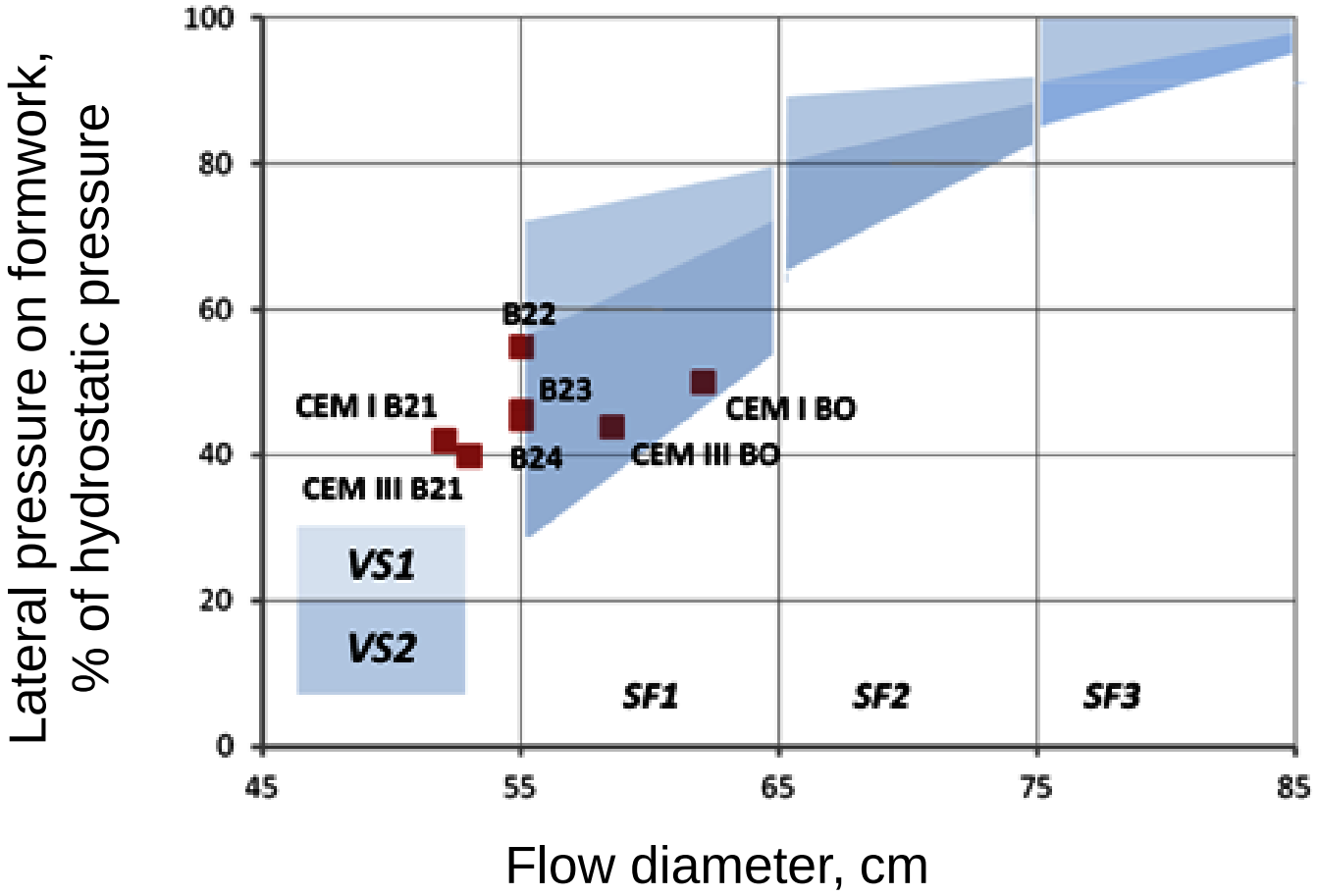

Density 2800-3500 kg/m^3
Aggregate: magnetite, serpentinite
Cement: CEM I, CEM III/A

Reduced air permeability for wet concrete

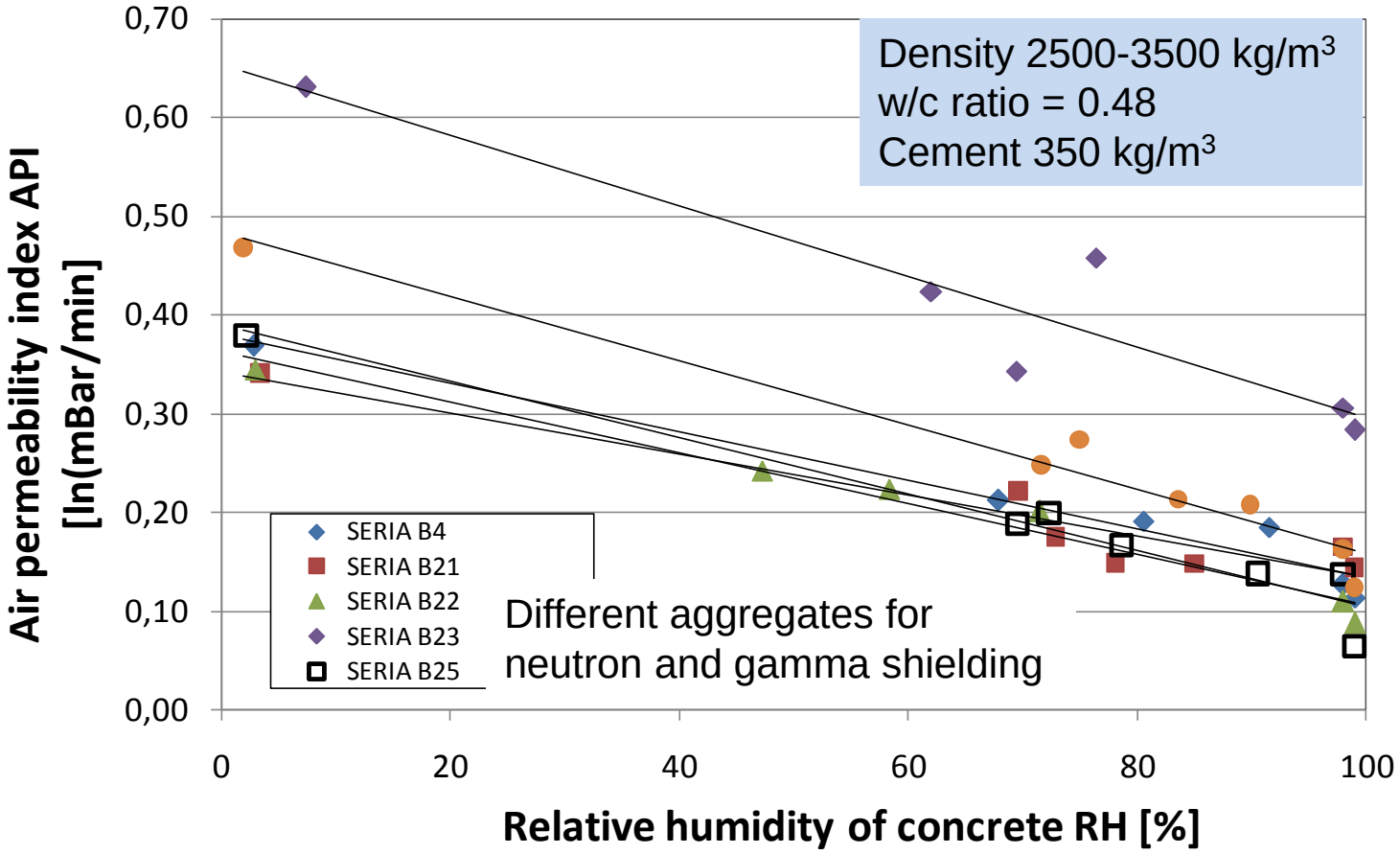

RH distribution in concrete

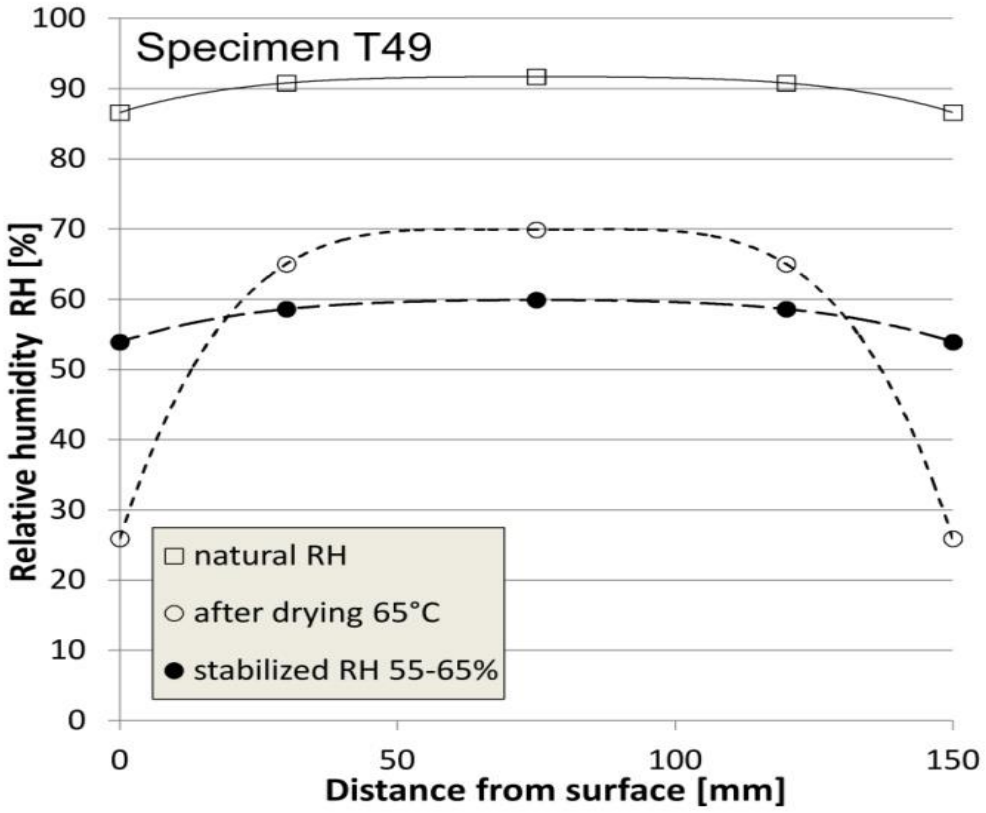

$$D_h = D_1\left[\alpha + \frac{1-\alpha}{1+\left[\left(1-RH\right)/\left(1-RH_C\right)\right]^n}\right]$$

Effect of boron compounds in cement setting and hardening

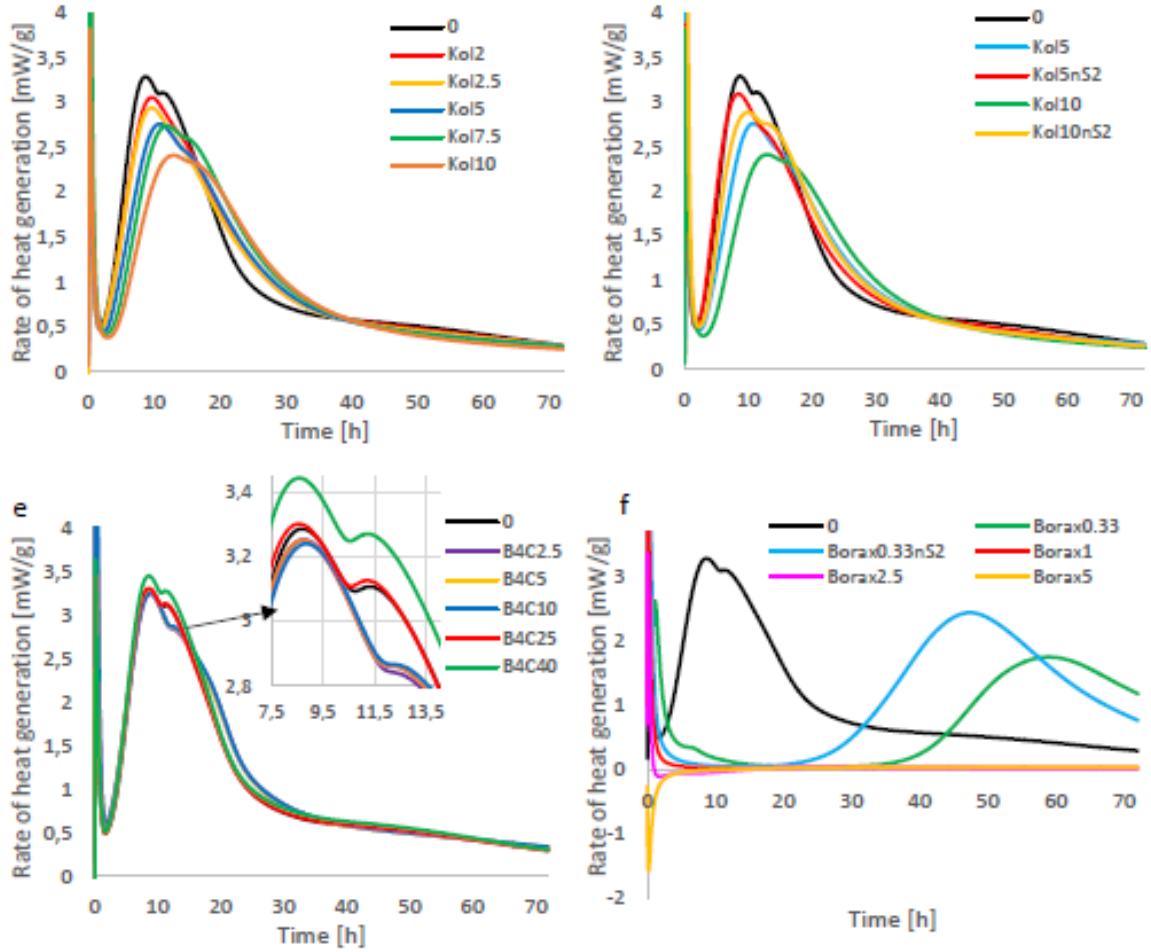

Fig. 1. The rate of heat generated per 1 g of cement during hydration of cement in mortar with different contents of (a) ulexite, (b) ulexite and nanosilica, (c) colemanite (d) colemanite and nanosilica, (e) boron carbide, (f) borax and nanosilica. Assumed notations: 0 - mortar without

Effect of boron compounds in cement setting and hardening

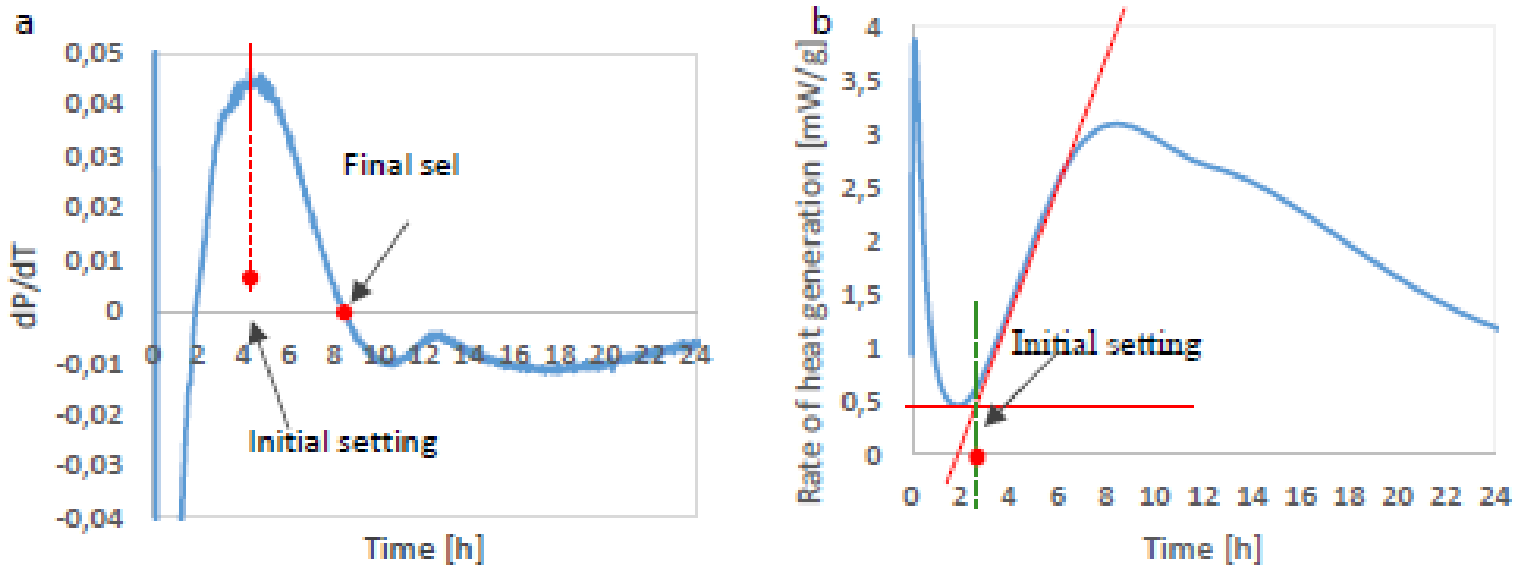

Fig. 4. Two concepts of the initial setting time determination: (a) the first derivative of the function of the rate of heat generation in time [20] (b) the point of intersection of tangent to the minimum and tangent to the point of inflection [21]

Ideas being consider:

1. Hardening concrete after the final cement set:

gamma radiation can enchance the microstructure development (further dissolution, localized heating→rate increase, …)

2. Hardened concrete:

- Moisture transport induced by radiation
- Dehydration of CSH

3. Concrete components

- Radiation induced transformation of minerals

dolomitic-limestone 1:1 with clay minerals; porosity

Ion implantation technique

Neutron induced transformation

4. Gamma/heat effects on the permebility of concrete

Long series of BMC conferences

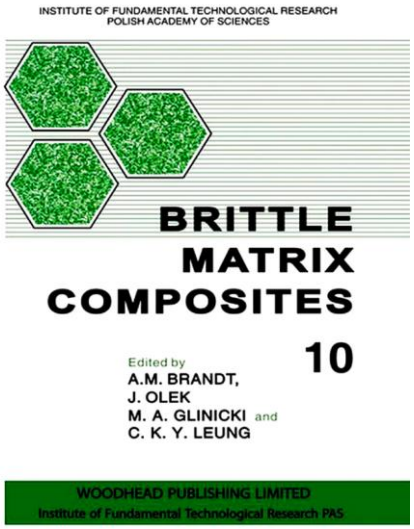

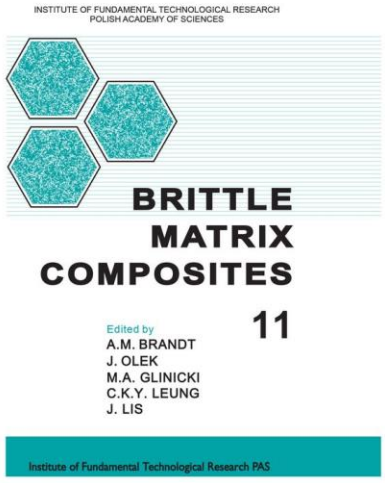

Proceedings from the BMC-9, BMC-10 and BMC-11 Conferences are indexed in the Web of Science

http://bmc.ippt.pan.pl/

https://www.sciencedirect.com/science/book/9780857099884

https://www.sciencedirect.com/science/book/9781845697754

Thank you for your attention!

Funding: The financial support by the National Centre for Research and Development (Project V4-Korea/2/2018) is gratefully acknowledged